PL-TN--92-1019

AD-A260 017

PL-TN--
92-1019

THE SINGLE-GAP HOLLOW SPHERICAL DIPOLE IN NON-CONDUCTING MEDIA

Carl E. Baum

January 1993

DTIC
ELECTE
JAN26 1993
S E D

APPROVED FOR PUBLIC RELEASE; DISTRIBUTION UNLIMITED.

93-01343

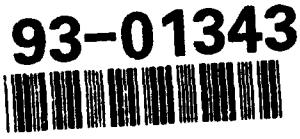

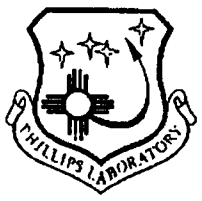

PHILLIPS LABORATORY
Advanced Weapons & Survivability Directorate
AIR FORCE MATERIEL COMMAND
KIRTLAND AIR FORCE BASE, NM 87117-6008

93 1 25 099

REPORT DOCUMENTATION PAGE

Form Approved
OMB No. 0704-0188

Public reporting burden for this collection of information is estimated to average 1 hour per response, including the time for reviewing instructions, searching existing data sources, gathering and maintaining the data needed, and completing and reviewing the collection of information. Send comments regarding this burden estimate or any other aspect of this collection of information, including suggestions for reducing this burden to Washington Headquarters Services, Directorate for information Operations and Reports, 1215 Jefferson Davis Highway, Suite 1204, Arlington, VA 22202-4302, and to the Office of Management and Budget, Paperwork Reduction Project (0704-0188), Washington, DC 20503.

1. AGENCY USE ONLY *(Leave blank)*	2. REPORT DATE	3. REPORT TYPE AND DATES COVERED
	January 1993	Technical Note

4. TITLE AND SUBTITLE

THE SINGLE-GAP HOLLOW SPHERICAL DIPOLE IN NON-CONDUCTING MEDIA

5. FUNDING NUMBERS

PR: 9993
TA: LA
WU: BS

6. AUTHOR(S)

Carl E. Baum

7. PERFORMING ORGANIZATION NAME(S) AND ADDRESS(ES)

8. PERFORMING ORGANIZATION REPORT NUMBER

9. SPONSORING / MONITORING AGENCY NAME(S) AND ADDRESS(ES)

Phillips Laboratory
Kirtland AFB, NM 87117-6008

10. SPONSORING / MONITORING AGENCY REPORT NUMBER

PL-TN--92-1019

11. SUPPLEMENTARY NOTES

Sensor and Simulation Notes, Note 91, 17 July 1969.
Publication of this report does not constitute approval or disapproval of the ideas or findings. It is published in the interest of scientific and technical*

12a. DISTRIBUTION / AVAILABILITY STATEMENT

Approved for public release; distribution unlimited.

12b. DISTRIBUTION CODE

13. ABSTRACT *(Maximum 200 words)*

This note considers the response of a hollow spherical dipole in non-conducting media. This sensor is a sphere with a slot around the equator which is uniformly resistively loaded. The current through the resistive load across the slot is proportional to the time rate of change of the displacement vector for low frequencies. The response characteristics of such a device at high frequencies are calculated using expansions in spherical wave functions. These calculations include the dependence of the sensor response on both frequency and the direction of wave incidence.

*information exchange. The established procedures for editing reports were not followed for this Technical Note.

14. SUBJECT TERMS

Hollow Spherical Dipole, Non-Conducting Media

15. NUMBER OF PAGES

72

16. PRICE CODE

17. SECURITY CLASSIFICATION OF REPORT	18. SECURITY CLASSIFICATION OF THIS PAGE	19. SECURITY CLASSIFICATION OF ABSTRACT	20. LIMITATION OF ABSTRACT
Unclassified	Unclassified	Unclassified	SAR

DTIC QUALITY INSPECTED 5

Accesion For
NTIS CRA&I
DTIC TAB
Unannounced
Justification
By
Distribution/
Availability Codes
Dist | Avail and/or Special
A-1

Sensor and Simulation Note
Note 91
17 July 1969

The Single-Gap Hollow Spherical Dipole in Non-Conducting Media

Capt Carl E. Baum
Air Force Weapons Laboratory

Abstract

This note considers the response of a hollow spherical dipole in non-conducting media. This sensor is a sphere with a slot around the equator which is uniformly resistively loaded. The current through the resistive load across the slot is proportional to the time rate of change of the displacement vector for low frequencies. The response characteristics of such a device at high frequencies are calculated using expansions in spherical wave functions. These calculations include the dependence of the sensor response on both frequency and the direction of wave incidence.

Foreword

The calculations in this note have a form similar to those in a few previous notes on cylindrical loops. This note extends these types of calculations to spherical geometries where the sensor in this case measures the displacement current density. For convenience the figures are grouped together after the summary and before the appendices. Appendix C was written by Mr. Joe P. Martinez of Dikewood and we would like to thank him and Mr. Larry Berg of AFWL for the numerical calculations and graphs.

Contents

I. Introduction

Among the problems of electromagnetic sensor design for use in non-conducting media there are the general problems of sensor accuracy, directional sensitivity at high frequencies, and maximizing the upper frequency response for a given sensitivity. Here we are concerned with sensors for measuring some electromagnetic field component, or its derivative, with a flat frequency response over the bandwidth of interest so that in measuring pulsed fields there is no distortion of the waveform, within limits like the risetime. As an example, a multi-gap cylindrical loop has a well calculable equivalent area for measuring a component of $\vec{B}$, and by increasing the number of gaps the upper frequency response can be raised and the directional sensitivity at high frequencies is reduced (for waves still propagating perpendicular to the loop axis).[1]

In this note we consider another kind of sensor which we term a hollow spherical dipole. Since this sensor is based on a sphere we can analyze its performance using vector eigenfunction expansions in spherical coordinates. (This in itself is a good reason for considering a spherical sensor.) The analysis will follow an approach similar to that used in two previous notes concerning cylindrical loops where cylindrical vector eigenfunctions were used.[1,2]

The basic sensor geometry is shown in figure 1. It consists of a hollow sphere of radius a with a gap of angular width $2\psi_o$ symmetrically cut around the equator of the sphere. The sensor is described in spherical coordinates (r, θ, ϕ) as a conducting surface on $r = a$ for $0 \leq \theta < \theta_o$ and $\pi - \theta_o < \theta \leq \pi$. The gap is described by $r = a$ and $\overline{\theta}_o < \theta < \pi - \theta_o$ where $0 \leq \theta_o < \pi/2$. We have the relation

$$\psi_o = \frac{\pi}{2} - \theta_o \tag{1}$$

There is also the cylindrical coordinate system (Ψ, ϕ, z) and the sensor geometry is constrained to have axial symmetry (about the z axis) so that its response is independent of ϕ. The gap is assumed to have resistive loading uniform in ϕ to preserve

1. Capt Carl E. Baum, Sensor and Simulation Note 41, The Multi-Gap Cylindrical Loop in Non-Conducting Media, May 1967.

2. Capt Carl E. Baum, Sensor and Simulation Note 30, The Single-Gap Cylindrical Loop in Non-Conducting and Conducting Media, January 1967.

axial symmetry. This resistive loading might in practice be many cable inputs evenly spaced around the gap; the cables would bring the total current crossing the gap with equal delays to one common point where the signal is desired. Such cable networks are not considered in this note, but they are assumed to be located in positions which do not significantly perturb the sensor geometry.

The basic mode of operation of this type of sensor uses the short circuit current across the loop gap. As will appear in the analysis, for wavelengths much larger than a the short circuit current is just $3\pi a^2$ times the z component of the total current density. If the medium conductivity is zero then the total current density is just the displacement current density. (There are no source currents in these calculations.) Thus one might refer to this sensor as a $\dot{D}$ sensor or a total current density sensor, depending on the specific application.[3] The sensor has an equivalent area of $3\pi a^2$ which is quite accurate as long as ψ_o is small. The actual accuracy of this number for the equivalent area is not considered in this note. The simplifying assumptions allowing the present high-frequency analysis give $3\pi a^2$ as the equivalent area.

In outline this note first considers the expansion of an incident electromagnetic plane wave in terms of spherical vector eigenfunctions. Then this plane wave is imposed on the sphere with a shorted gap in order to calculate the short circuit current as a function of frequency and the angle of wave incidence. Then assuming small ψ_o and a quasi static electric field distribution across the gap we calculate the sensor admittances associated with both the volume inside and outside the sensor. Combining the admittances due to the sensor geometry and the assumed cable loading with the short circuit current then gives the sensor response functions for an incident plane wave. From these results things like optimum cable loading can be calculated. For this sensor with the case of interest that the medium conductivity is zero the admittance due to the cable loading is large compared to the sensor admittance (basically a capacitance) for frequencies below the upper frequency response of the sensor. The sensor response is then normalized by dividing the current output by $3\pi a^2$ times $\dot{D}$, the ideal low-frequency response.

3. Capt Carl E. Baum, Sensor and Simulation Note 38, Parameters for Some Electrically-Small Electromagnetic Sensors, March 1967.

II. Electromagnetic Fields in Spherical Coordinates

Consider that we have a linear, homogeneous, isotropic medium with permittivity ε, permeability μ, and conductivity σ. We have propagation constants[4]

$$k = \sqrt{-i\omega\mu(\sigma + i\omega\varepsilon)}$$

$$\gamma = \sqrt{s\mu(\sigma + s\varepsilon)} \tag{2}$$

and a wave impedance

$$Z = \sqrt{\frac{s\mu}{\sigma + s\varepsilon}} = \sqrt{\frac{i\omega\mu}{\sigma + i\omega\varepsilon}} \tag{3}$$

where s is the Laplace transform variable which we take as $i\omega$ for the frequency-domain analysis in this note. The radian frequency is ω and i is the unit imaginary. Our interest lies for the most part in $\sigma = 0$, as is used for the numerical calculations. However we keep σ in the analysis for generality.

With time harmonic fields and with $e^{i\omega t}$ suppressed Maxwell's equations have the form

$$\nabla \times \vec{E} = -i\omega\vec{B}\ , \qquad \nabla \times \vec{H} = \vec{J} + i\omega\vec{D}$$

$$\nabla \cdot \vec{B} = 0\ , \qquad \nabla \cdot \vec{D} = \rho \tag{4}$$

together with the constitutive relations and Ohm's law

$$\vec{B} = \mu\vec{H}\ , \qquad \vec{D} = \varepsilon\vec{E}\ , \qquad \vec{J} = \sigma\vec{E} \tag{5}$$

From equations 4 and 5 one obtains vector wave equations of the form

$$\nabla^2\vec{E} + k^2\vec{E} = \vec{0}\ , \qquad \nabla^2\vec{H} + k^2\vec{H} = \vec{0} \tag{6}$$

Note that there are assumed to be no source currents or charges ($\rho = 0$) in the medium, but there will be charges (and currents) on the spherical sensor. Thus $\vec{E}$ (as well as $\vec{H}$) has zero divergence away from boundaries allowing the result in equations 6.

4. All units are rationalized MKSA.

In spherical coordinates the solution of the scalar wave equation can be written as a linear combination of functions of the form[5]

$$\Xi^{(\ell)}(n, m, \begin{matrix} e \\ o \end{matrix}) \equiv f_n^{(\ell)}(kr) P_n^m(\cos(\theta)) \begin{Bmatrix} \cos(m\phi) \\ \sin(m\phi) \end{Bmatrix} \tag{7}$$

where $f_n^{(\ell)}(kr)$ is one of the spherical Bessel functions $j_n(kr)$, $y_n(kr)$, $h_n^{(1)}(kr)$, $h_n^{(2)}(kr)$ for $\ell = 1, 2, 3, 4$ in that order. The third argument of Ξ is listed as e or o (meaning even or odd); e corresponds to using $\cos(m\phi)$ and o to using $\sin(m\phi)$. Unless noted to the contrary the definitions of the special functions correspond to those in a standard reference work.[6] In particular the Legendre functions of the first kind $P_n^m(\xi)$ of degree n and order m on the cut $(-1 \leq \xi \leq 1)$ in the complex ξ plane have the form (ref. 6 eqn. 8.6.6)

$$P_n^m(\xi) \equiv (-1)^m (1 - \xi^2)^{\frac{m}{2}} \frac{d^m}{d\xi^m} P_n(\xi) \tag{8}$$

where

$$P_n(\xi) \equiv P_n^o(\xi) \equiv \frac{1}{2^n n!} \frac{d^n}{d\xi^n} (\xi^2 - 1)^n \tag{9}$$

where we only consider n and m as non negative integers and ξ as a real argument with $-1 \leq \xi \leq 1$. Our definition differs from that in some texts on electromagnetic theory[5,7,8] in which the factor of $(-1)^m$ is not included. The form of equation 8 is however consistent with various texts dealing with the special

5. J. A. Stratton, Electromagnetic Theory, McGraw Hill, 1941, section 7.3.

6. Abramowitz and Stegun, ed., Handbook of Mathematical Functions, AMS 55, National Bureau of Standards, 1964.

7. W. R. Smythe, Static and Dynamic Electricity, 2nd. ed., McGraw Hill, 1950.

8. Morse and Feshbach, Methods of Theoretical Physics, McGraw Hill, 1953.

functions of mathematical physics.[6,9,10] For ξ as a general complex number not on the cut ($-1 \leq \xi \leq 1$) the definition differs somewhat. The form in equation 8 agrees with more general definitions for real m not necessarily an integer. In any case we only use $-1 \leq \xi \leq 1$ in this note.

Similar to Stratton (ref. 5, section 7.11) define two independent sets of vector wave functions which can be used to construct any divergenceless vector field satisfying the vector wave equation (as in equations 6). The first set of vector wave functions is defined by

$$\vec{M}^{(\ell)}(n, m, \begin{matrix} e \\ o \end{matrix}) \equiv \nabla \times \left[r \Xi^{(\ell)}(n, m, \begin{matrix} e \\ o \end{matrix}) \vec{e}_r \right] \tag{10}$$

where $\vec{e}_r$ is the unit vector in the r direction, and similarly for other unit vectors. These vector wave functions have components as

$$M_r^{(\ell)}(n, m, \begin{matrix} e \\ o \end{matrix}) = 0$$

$$M_\theta^{(\ell)}(n, m, \begin{matrix} e \\ o \end{matrix}) = \frac{1}{\sin(\theta)} \frac{\partial}{\partial \phi} \Xi^{(\ell)}(n, m, \begin{matrix} e \\ o \end{matrix}) \tag{11}$$

$$M_\phi^{(\ell)}(n, m, \begin{matrix} e \\ o \end{matrix}) = - \frac{d}{d\theta} \Xi^{(\ell)}(n, m, \begin{matrix} e \\ o \end{matrix})$$

where the last two components can be expanded as

$$M_\theta^{(\ell)}(n, m, \begin{matrix} e \\ o \end{matrix}) = f_n^{(\ell)}(kr) \frac{P_n^m(\cos(\theta))}{\sin(\theta)} m \begin{vmatrix} -\sin(m\phi) \\ \cos(m\phi) \end{vmatrix}$$

$$M_\phi^{(\ell)}(n, m, \begin{matrix} e \\ o \end{matrix}) = -f_n^{(\ell)}(kr) \frac{dP_n^m(\cos(\theta))}{d\theta} \begin{vmatrix} \cos(m\phi) \\ \sin(m\phi) \end{vmatrix} \tag{12}$$

9. Magnus, Oberhettinger, and Soni, Formulas and Theorems for the Special Functions of Mathematical Physics, 3rd ed., Springer-Verlag New York, 1966.

10. E. W. Hobson, The Theory of Spherical and Ellipsoidal Harmonics, Chelsea, New York, 1955.

The second set of vector wave functions is defined by

$$\vec{N}^{(\ell)}(n, m, \begin{matrix} e \\ o \end{matrix}) \equiv \frac{1}{k} \nabla \times \vec{M}^{(\ell)}(n, m, \begin{matrix} e \\ o \end{matrix}) \tag{13}$$

which has components

$$N_r^{(\ell)}(n, m, \begin{matrix} e \\ o \end{matrix}) = \frac{n(n+1)}{kr} \Xi^{(\ell)}(n, m, \begin{matrix} e \\ o \end{matrix})$$

$$N_\theta^{(\ell)}(n, m, \begin{matrix} e \\ o \end{matrix}) = \frac{1}{kr} \frac{\partial^2}{\partial(kr)\partial\theta}\left[kr\Xi^{(\ell)}(n, m, \begin{matrix} e \\ o \end{matrix})\right] \tag{14}$$

$$N_\phi^{(\ell)}(n, m, \begin{matrix} e \\ o \end{matrix}) = \frac{1}{kr \sin(\theta)} \frac{\partial^2}{\partial(kr)\partial\phi}\left[kr\Xi^{(\ell)}(n, m, \begin{matrix} e \\ o \end{matrix})\right]$$

which can be expanded as

$$N_r^{(\ell)}(n, m, \begin{matrix} e \\ o \end{matrix}) = n(n+1) \frac{f_n^{(\ell)}(kr)}{kr} P_n^m(\cos(\theta)) \begin{Bmatrix} \cos(m\phi) \\ \sin(m\phi) \end{Bmatrix}$$

$$N_\theta^{(\ell)}(n, m, \begin{matrix} e \\ o \end{matrix}) = \frac{\left[krf_n^{(\ell)}(kr)\right]'}{kr} \frac{dP_n^m(\cos(\theta))}{d\theta} \begin{Bmatrix} \cos(m\phi) \\ \sin(m\phi) \end{Bmatrix} \tag{15}$$

$$N_\phi^{(\ell)}(n, m, \begin{matrix} e \\ o \end{matrix}) = \frac{\left[krf_n^{(\ell)}(kr)\right]'}{kr} \frac{P_n^m(\cos(\theta))}{\sin(\theta)} m \begin{Bmatrix} -\sin(m\phi) \\ \cos(m\phi) \end{Bmatrix}$$

where a prime is used to indicate differentiation with respect to the argument of the spherical Bessel function being considered. Similar to equation 13 we also have the relation

$$\vec{M}^{(\ell)}(n, m, \begin{matrix} e \\ o \end{matrix}) = \frac{1}{k} \nabla \times \vec{N}^{(\ell)}(n, m, \begin{matrix} e \\ o \end{matrix}) \tag{16}$$

The $\vec{N}$ and $\vec{M}$ functions are mutually orthogonal on a sphere (of constant kr). Also on the unit sphere we have the orthogonality relations that two $\vec{N}$ functions with different n or m are orthogonal, or if one is even and the other odd they are orthogonal. The

same results hold for the $\vec{M}$ functions. For all indices the same we have

$$\int_0^{2\pi}\int_0^{\pi} \vec{M}^{(\ell)}(n, m, \begin{matrix}e\\o\end{matrix}) \cdot \vec{M}^{(\ell)}(n, m, \begin{matrix}e\\o\end{matrix}) \sin(\theta)d\theta d\phi$$

$$= [1 \pm \delta_{m,o}] 2\pi \frac{n(n+1)}{2n+1} \frac{(n+m)!}{(n-m)!} \left[f_n^{(\ell)}(kr)\right]^2 \qquad (17)$$

and

$$\int_0^{2\pi}\int_0^{\pi} \vec{N}^{(\ell)}(n, m, \begin{matrix}e\\o\end{matrix}) \cdot \vec{N}^{(\ell)}(n, m, \begin{matrix}e\\o\end{matrix}) \sin(\theta)d\theta d\phi$$

$$= [1 \pm \delta_{m,o}] 2\pi \frac{n(n+1)}{(2n+1)^2} \frac{(n+m)!}{(n-m)!}$$

$$\cdot \left\{ (n+1)\left[f_{n-1}^{(\ell)}(kr)\right]^2 + n\left[f_{n+1}^{(\ell)}(kr)\right]^2 \right\} \qquad (18)$$

where δ_{m_1,m_2} is the Kronecker delta function defined by

$$\delta_{m_1,m_2} \equiv \begin{cases} 1 & \text{for } m_1 = m_2 \\ 0 & \text{for } m_1 \neq m_2 \end{cases} \qquad (19)$$

With the $\vec{N}$ and $\vec{M}$ vector wave functions we can now expand an electric field with zero divergence as

$$\vec{E} = E_o \sum_{n=o}^{\infty} \sum_{m=o}^{n} \left| \alpha_{n,m} \vec{M}^{(\ell)}(n, m, \begin{matrix}e\\o\end{matrix}) + \beta_{n,m} \vec{N}^{(\ell)}(n, m, \begin{matrix}e\\o\end{matrix}) \right| \qquad (20)$$

where E_o is some constant with dimensions volts/meter and where $\alpha_{n,m}$ and $\beta_{n,m}$ are dimensionless constants. Note that we can also sum over ℓ and over even and odd functions but typically for some particular form of wave only one ℓ will be needed and with appropriate symmetry only one of e and o will be needed for each type of vector wave function. Comparing equations 4 and 5 with the

relations between the $\vec{M}$ and $\vec{N}$ functions (equations 13 and 16) note that we can find $\vec{H}$ from $\vec{E}$ by replacing

$$\vec{M}^{(\ell)}(n, m, \begin{matrix} e \\ o \end{matrix}) \rightarrow \frac{i}{Z}\vec{N}^{(\ell)}(n, m, \begin{matrix} e \\ o \end{matrix})$$

$$\vec{N}^{(\ell)}(n, m, \begin{matrix} e \\ o \end{matrix}) \rightarrow \frac{i}{Z}\vec{M}^{(\ell)}(n, m, \begin{matrix} e \\ o \end{matrix}) \qquad (21)$$

giving an $\vec{H}$ to go with equation 20 as

$$\vec{H} = i\frac{E_o}{Z}\sum_{n=o}^{\infty}\sum_{m=o}^{n}\left|\alpha_{n,m}\vec{N}^{(\ell)}(n, m, \begin{matrix} e \\ o \end{matrix}) + \beta_{n,m}\vec{M}^{(\ell)}(n, m, \begin{matrix} e \\ o \end{matrix})\right| \qquad (22)$$

Similarly if we are given an expansion for $\vec{H}$ we can find $\vec{E}$ by substituting

$$\vec{M}^{(\ell)}(n, m, \begin{matrix} e \\ o \end{matrix}) \rightarrow -iZ\vec{N}^{(\ell)}(n, m, \begin{matrix} e \\ o \end{matrix})$$

$$\vec{N}^{(\ell)}(n, m, \begin{matrix} e \\ o \end{matrix}) \rightarrow -iZ\vec{M}^{(\ell)}(n, m, \begin{matrix} e \\ o \end{matrix}) \qquad (23)$$

With the $\vec{N}$ and $\vec{M}$ functions we can expand any electromagnetic field distribution as long as the fields have no divergence which requires $\rho = 0$ in equations 4. For completeness note that the wave equation for $\vec{E}$ found from equations 4 and 5 is

$$-\nabla \times (\nabla \times \vec{E}) + k^2\vec{E} = 0 \qquad (24)$$

which reduces to

$$\nabla^2\vec{E} - \nabla(\nabla \cdot \vec{E}) + k^2\vec{E} = 0 \qquad (25)$$

As discussed by Stratton another set of wave functions are needed which we define as

$$\vec{L}^{(\ell)}(n, m, \begin{matrix} e \\ o \end{matrix}) \equiv \frac{1}{k}\nabla\Xi^{(\ell)}(n, m, \begin{matrix} e \\ o \end{matrix}) \qquad (26)$$

which has components

$$L_r^{(\ell)}(n, m, \begin{matrix} e \\ o \end{matrix}) = f_n^{(\ell)\prime}(kr) P_n^m(\cos(\theta)) \begin{Bmatrix} \cos(m\phi) \\ \sin(m\phi) \end{Bmatrix}$$

$$L_\theta^{(\ell)}(n, m, \begin{matrix} e \\ o \end{matrix}) = \frac{f_n^{(\ell)}(kr)}{kr} \frac{dP_n^m(\cos(\theta))}{d\theta} \begin{Bmatrix} \cos(m\phi) \\ \sin(m\phi) \end{Bmatrix} \tag{27}$$

$$L_\phi^{(\ell)}(n, m, \begin{matrix} e \\ o \end{matrix}) = \frac{f_n^{(\ell)}(kr)}{kr} \frac{P_n^m(\cos(\theta))}{\sin(\theta)} m \begin{Bmatrix} -\sin(m\phi) \\ \cos(m\phi) \end{Bmatrix}$$

The $\vec{L}$ and $\vec{M}$ vector functions are related as

$$\vec{M}^{(\ell)}(n, m, \begin{matrix} e \\ o \end{matrix}) = kr\vec{L}^{(\ell)}(n, m, \begin{matrix} e \\ o \end{matrix}) \times \vec{e}_r \tag{28}$$

The $\vec{L}$ and $\vec{M}$ functions are mutually orthogonal on a sphere (of constant kr). However the $\vec{L}$ and $\vec{N}$ functions are only orthogonal if at least one of the indices $(\ell, n, m, \begin{matrix} e \\ o \end{matrix})$ differs. The $\vec{L}$ functions are orthogonal to each other unless the indices are all the same, in which case we have

$$\int_0^{2\pi} \int_0^{\pi} \vec{L}^{(\ell)}(n, m, \begin{matrix} e \\ o \end{matrix}) \cdot \vec{L}^{(\ell)}(n, m, \begin{matrix} e \\ o \end{matrix}) \sin(\theta) d\theta d\phi$$

$$= [1 \pm \delta_{m,o}] \frac{2\pi}{2n+1} \frac{(n+m)!}{(n-m)!} \left\{ \left[f_n^{(\ell)\prime}(kr) \right]^2 \right.$$

$$\left. + \frac{n(n+1)}{(kr)^2} \left[f_n^{(\ell)}(kr) \right]^2 \right\} \tag{29}$$

For another reference concerning these spherical vector wave functions see Morse and Feshback.[11] The definitions used here are similar to Morse and Feshback except that we use $e^{i\omega t}$ whereas Stratton and Morse and Feshback both use $e^{-i\omega t}$ for the harmonic time dependence.

11. Ref. 8, Part II, pp. 1864-1866.

III. Vector Plane Waves in Spherical Coordinates

Now consider vector plane waves in spherical coordinates. Such a wave has the general form

$$\vec{F} \equiv F_o \vec{u} e^{-i\vec{k}\cdot\vec{r}} \tag{30}$$

where $\vec{u}$ is some unit vector with fixed direction and where the propagation vector is given by

$$\vec{k} \equiv k\vec{e}_1 \tag{31}$$

where $\vec{e}_1$ is the direction of propagation of the wave. Figure 2A shows a general plane wave at some position $\vec{r}$ propagating in the $\vec{e}_1$ direction with $\vec{E}$, $\vec{H}$, and $\vec{k}$ all mutually orthogonal vectors. We assume that $\vec{E}$ has a fixed polarization (and thus $\vec{H}$ also has a fixed polarization) for purposes of illustration. This plane wave also has

$$\vec{E} = Z\vec{H} \times \vec{e}_1 \tag{32}$$

so that the wave is propagating in the $+\vec{e}_1$ direction.

$\vec{e}_1$ is a fixed direction in space determining the direction of wave propagation. $\vec{E}$ and $\vec{H}$ are parallel to a plane which is in turn perpendicular to $\vec{e}_1$. Construct two orthogonal unit vectors, $\vec{e}_2$ and $\vec{e}_3$, parallel to this plane as shown in figure 2B. Now since $\vec{e}_1$ is a fixed direction in space it can be described by fixed angles θ_1 and ϕ_1 in a spherical coordinate system with respect to the cartesian unit vectors $(\vec{e}_x, \vec{e}_y, \vec{e}_z)$ which are also fixed directions in space. As shown in figure 2B choose $\vec{e}_2$ to be parallel to the same plane to which both $\vec{e}_1$ and $\vec{e}_z$ are parallel; also make $\vec{e}_2$ perpendicular to $\vec{e}_1$. Finally choose $\vec{e}_3$ perpendicular to both $\vec{e}_1$ and $\vec{e}_2$, thereby making it parallel to the x, y plane.

These new unit vectors are made to form a right handed system so that we have

$$\vec{e}_1 \times \vec{e}_2 = \vec{e}_3 , \qquad \vec{e}_2 \times \vec{e}_3 = \vec{e}_1 , \qquad \vec{e}_3 \times \vec{e}_1 = \vec{e}_2 \tag{33}$$

Note that $\vec{e}_2$ is chosen such that for $0 < \theta_1 < \pi/2$ the polar angle of $\vec{e}_2$ is $\pi/2 - \theta_1$. In terms of the cartesian unit vectors we have

$$\vec{e}_1 = \sin(\theta_1)\cos(\phi_1)\vec{e}_x + \sin(\theta_1)\sin(\phi_1)\vec{e}_y + \cos(\theta_1)\vec{e}_z$$

$$\vec{e}_2 = -\cos(\theta_1)\cos(\phi_1)\vec{e}_x - \cos(\theta_1)\sin(\phi_1)\vec{e}_y + \sin(\theta_1)\vec{e}_z \quad (34)$$

$$\vec{e}_3 = \sin(\phi_1)\vec{e}_x - \cos(\phi_1)\vec{e}_y$$

Cartesian and spherical coordinates are related as

$$x = r\sin(\theta)\cos(\phi)$$

$$y = r\sin(\theta)\sin(\phi) \quad (35)$$

$$z = r\cos(\theta)$$

The cartesian and spherical unit vectors are related as

$$\vec{e}_x = \sin(\theta)\cos(\phi)\vec{e}_r + \cos(\theta)\cos(\phi)\vec{e}_\theta - \sin(\phi)\vec{e}_\phi$$

$$\vec{e}_y = \sin(\theta)\sin(\phi)\vec{e}_r + \cos(\theta)\sin(\phi)\vec{e}_\theta + \cos(\phi)\vec{e}_\phi \quad (36)$$

$$\vec{e}_z = \cos(\theta)\vec{e}_r - \sin(\theta)\vec{e}_\theta$$

or

$$\vec{e}_r = \sin(\theta)\cos(\phi)\vec{e}_x + \sin(\theta)\sin(\phi)\vec{e}_y + \cos(\theta)\vec{e}_z$$

$$\vec{e}_\theta = \cos(\theta)\cos(\phi)\vec{e}_x + \cos(\theta)\sin(\phi)\vec{e}_y - \sin(\theta)\vec{e}_z \quad (37)$$

$$\vec{e}_\phi = -\sin(\phi)\vec{e}_x + \cos(\phi)\vec{e}_y$$

Substitute for the cartesian unit vectors in equations 34 from equations 36 and use some trigonometric identities to give

$$\vec{e}_1 = [\cos(\theta_1)\cos(\theta) + \sin(\theta_1)\sin(\theta)\cos(\phi - \phi_1)]\vec{e}_r$$

$$+ [-\cos(\theta_1)\sin(\theta) + \sin(\theta_1)\cos(\theta)\cos(\phi - \phi_1)]\vec{e}_\theta$$

$$- \sin(\theta_1)\sin(\phi - \phi_1)\vec{e}_\phi$$

$$\vec{e}_2 = [\sin(\theta_1)\cos(\theta) - \cos(\theta_1)\sin(\theta)\cos(\phi - \phi_1)]\vec{e}_r$$

$$- [\sin(\theta_1)\sin(\theta) + \cos(\theta_1)\cos(\theta)\cos(\phi - \phi_1)]\vec{e}_\theta \qquad (38)$$

$$+ \cos(\theta_1)\sin(\phi - \phi_1)\vec{e}_\phi$$

$$\vec{e}_3 = -\sin(\theta)\sin(\phi - \phi_1)\vec{e}_r$$

$$-\cos(\theta)\sin(\phi - \phi_1)\vec{e}_\theta$$

$$-\cos(\phi - \phi_1)\vec{e}_\phi$$

Note that ϕ and ϕ_1 appear in the combination $\phi - \phi_1$ in this formulation.

The general unit vector $\vec{u}$ (with constant direction) used in equation 30 can be considered as a linear combination of the system of orthogonal unit vectors $\vec{e}_1$, $\vec{e}_2$, $\vec{e}_3$. Now $\vec{e}_1$ gives the direction of propagation of the vector plane wave. For our purposes we have an electromagnetic wave which is an assumed TEM plane wave. This plane wave will be used as the incident wave for calculating the sensor response. Calling the electric field $\vec{E}_{inc}$ and the magnetic field $\vec{H}_{inc}$ then $\vec{E}_{inc}$ and $\vec{H}_{inc}$ must both be perpendicular to $\vec{e}_1$; they can then be formed from linear combinations of $\vec{e}_1$ and $\vec{e}_2$. In figure 3 we illustrate such a plane wave incident on a sphere centered on $\vec{r} = \vec{0}$. The slot around the sphere is to be centered on $\theta = \pi/2$ so as to make the sensor symmetric with respect to the x, y plane. By symmetry if $\vec{E}_{inc}$ were parallel to $\vec{e}_2$ and thus parallel to the x, y plane it would drive no net current across the gap; note we are going to integrate the current all around the gap to obtain the short-circuit current for the sensor. Thus we are only interested in the polarization of

the incident wave for which $\vec{E}_{inc}$ is parallel to $\vec{e}_2$ and our incident wave is defined by

$$\vec{E}_{inc} \equiv E_o \vec{e}_2 e^{-i\vec{k}\cdot\vec{r}}$$

$$\vec{H}_{inc} \equiv \frac{E_o}{Z} \vec{e}_3 e^{-i\vec{k}\cdot\vec{r}} \tag{39}$$

Since one can convert an electric field distribution to the associated magnetic field by the transformations in equations 21 we only need to expand $\vec{E}_{inc}$ in terms of the $\vec{M}$ and $\vec{N}$ functions; $\vec{H}_{inc}$ is directly obtainable from the expansion of $\vec{E}_{inc}$.

As a further simplification we will later set $\phi_1 = 0$ to make $\vec{k}$ parallel to the x, z plane as shown in figure 3. Since the sensor geometry is independent of ϕ this represents no loss in generality. Consider an r_1, θ_1, ϕ_1 spherical coordinate system where θ_1 and ϕ_1 are the angles fixing the direction of propagation of the incident plane wave as above. The unit vectors for such a coordinate system are

$$\vec{e}_{r_1} \equiv \vec{e}_1 , \qquad \vec{e}_{\theta_1} \equiv -\vec{e}_2 , \qquad \vec{e}_{\phi_1} \equiv -\vec{e}_3 \tag{40}$$

As in Morse and Feshback[12] we define vector spherical harmonics using the spherical angles θ_1, ϕ_1 as

$$\vec{P}(n, m, \begin{matrix} e \\ o \end{matrix}) \equiv \vec{e}_{r_1} P_n^m(\cos(\theta_1)) \begin{Vmatrix} \cos(m\phi_1) \\ \sin(m\phi_1) \end{Vmatrix}$$

$$\vec{B}(n, m, \begin{matrix} e \\ o \end{matrix}) \equiv \frac{\sqrt{n(n+1)}}{(2n+1)\sin(\theta_1)} \left\{ \vec{e}_{\theta_1} \left[\frac{n-m+1}{n+1} P_{n+1}^m(\cos(\theta_1)) \right.\right.$$

$$\left. - \frac{n+m}{n} P_{n-1}^m(\cos(\theta_1)) \right] \begin{Vmatrix} \cos(m\phi_1) \\ \sin(m\phi_1) \end{Vmatrix}$$

$$\left. + \vec{e}_{\phi_1} \frac{m(2n+1)}{n(n+1)} P_n^m(\cos(\theta_1)) \begin{Vmatrix} -\sin(m\phi_1) \\ \cos(m\phi_1) \end{Vmatrix} \right\}$$

12. Ref. 8, Part II, pp. 1898, 1899.

$$\vec{C}(n,\ m,\ \begin{matrix}e\\o\end{matrix}) \equiv \frac{\sqrt{n(n+1)}}{(2n+1)\sin(\theta_1)}\left\{\vec{e}_{\theta_1}\ \frac{m(2n+1)}{n(n+1)}\ P_n^m(\cos(\theta_1))\left\{\begin{matrix}-\sin(m\phi_1)\\ \\ \cos(m\phi_1)\end{matrix}\right.\right.$$

$$-\ \vec{e}_{\phi_1}\left[\frac{n-m+1}{n+1}\ P_{n+1}^m(\cos(\theta_1))\right.$$

$$\left.\left.-\ \frac{n+m}{n}\ P_{n-1}^m(\cos(\theta_1))\right]\left\{\begin{matrix}\cos(m\phi_1)\\ \\ \sin(m\phi_1)\end{matrix}\right.\right\} \qquad (41)$$

The letters e and o refer to even and odd functions and are associated with the upper and lower functions in braces just as with the vector wave functions previously introduced.

Now we introduce the result of Morse and Feshback[13] for a dyadic plane wave with i switched to -i giving

$$(\delta_{\alpha,\beta})e^{-i\vec{k}\cdot\vec{r}} = \begin{pmatrix}1 & 0 & 0\\ 0 & 1 & 0\\ 0 & 0 & 1\end{pmatrix}e^{-i\vec{k}\cdot\vec{r}}$$

$$= \sum_{n=o}^{\infty}\sum_{m=o}^{n}\sum_{e,o}[2-\delta_{m,o}](-i)^n(2n+1)\ \frac{(n-m)!}{(n+m)!}\left\{i\vec{P}(n,m,\begin{matrix}e\\o\end{matrix})\vec{L}^{(1)}(n,m,\begin{matrix}e\\o\end{matrix})\right.$$

$$\left.+\ \frac{1}{\sqrt{n(n+1)}}\left[\vec{C}(n,m,\begin{matrix}e\\o\end{matrix})\vec{M}^{(1)}(n,m,\begin{matrix}e\\o\end{matrix})\ +\ i\vec{B}(n,m,\begin{matrix}e\\o\end{matrix})\vec{N}^{(1)}(n,m,\begin{matrix}e\\o\end{matrix})\right]\right\} \qquad (42)$$

The $\vec{P}$, $\vec{B}$, $\vec{C}$ vector spherical harmonics are functions of θ_1 and ϕ_1 while the $\vec{L}$, $\vec{M}$, $\vec{N}$ spherical vector wave functions are functions of r, θ, and ϕ. Note the use of dyadic notation where two vectors are written side by side to form a dyadic. $(\delta_{\alpha,\beta})$ is the identity dyadic which is also written in matrix form in equation 42. A vector plane wave is formed by taking the dot product of some constant vector on the left of the terms in equation 42. Using a general unit vector $\vec{u}$ with fixed direction (as in equation 30) we have a vector plane wave as

13. Ref. 8, Part II, p. 1866.

$$\vec{u}e^{-i\vec{k}\cdot\vec{r}} = \vec{u} \cdot (\delta_{\alpha,\beta})e^{-i\vec{k}\cdot\vec{r}}$$

$$= \sum_{n=o}^{\infty} \sum_{m=o}^{n} \sum_{e,o} [2-\delta_{m,o}](-i)^n(2n+1) \frac{(n-m)!}{(n+m)!} \left\{ i[\vec{u}\cdot\vec{P}(n,m,\overset{e}{o})]\vec{L}^{(1)}(n,m,\overset{e}{o}) \right.$$

$$\left. + \frac{1}{\sqrt{n(n+1)}} \left[[\vec{u}\cdot\vec{C}(n,m,\overset{e}{o})]\vec{M}^{(1)}(n,m,\overset{e}{o}) + i[\vec{u}\cdot\vec{B}(n,m,\overset{e}{o})]\vec{N}^{(1)}(n,m,\overset{e}{o}) \right] \right\} \tag{43}$$

The problem of expanding a vector plane wave then reduces to finding the coefficients expressed above as dot products.

Our plane wave of interest (equations 39) can be found by setting $\vec{u}$ equal to $\vec{e}_2$ and then equal to $\vec{e}_3$ while using the relations for $\vec{e}_2$ and $\vec{e}_3$ given in equations 40 and setting $\phi_1 = 0$. Considering first $\vec{e}_2$ we have

$$i\vec{e}_2 \cdot \vec{P}(n, m, \overset{e}{o}) = -i\vec{e}_{\theta_1} \cdot \vec{P}(n, m, \overset{e}{o}) = 0$$

$$\frac{1}{\sqrt{n(n+1)}} \vec{e}_2 \cdot \vec{C}(n, m, \overset{e}{o}) = \frac{-1}{\sqrt{n(n+1)}} \vec{e}_{\theta_1} \cdot \vec{C}(n, m, \overset{e}{o})$$

$$= - \frac{1}{\sin(\theta_1)} \frac{m}{n(n+1)} P_n^m(\cos(\theta_1)) \begin{Bmatrix} 0 \\ 1 \end{Bmatrix} \tag{44}$$

$$\frac{i}{\sqrt{n(n+1)}} \vec{e}_2 \cdot \vec{B}(n, m, \overset{e}{o}) = \frac{-i}{\sqrt{n(n+1)}} \vec{e}_{\theta_1} \cdot \vec{B}(n, m, \overset{e}{o})$$

$$= \frac{-i}{\sin(\theta_1)} \frac{1}{2n+1} \left[\frac{n-m+1}{n+1} P_{n+1}^m(\cos(\theta_1)) - \frac{n+m}{n} P_{n-1}^m(\cos(\theta_1)) \right] \begin{Bmatrix} 1 \\ 0 \end{Bmatrix}$$

Thus only the second set of coefficients for odd harmonics and the third set for even harmonics can be non zero. Note that $n = 0$ is not used because the corresponding $\vec{M}$ and $\vec{N}$ functions are identically zero. The last of equations 44 can be rewritten using identities for the Legendre functions[14] as

14. Ref. 5, p. 402.

$$\frac{i}{\sqrt{n(n+1)}}\,\vec{e}_2 \cdot \vec{B}(n,\,m,\,{}^{e}_{o}) = \frac{-i}{n(n+1)}\,\frac{dP_n^m(\cos(\theta_1))}{d\theta_1}\begin{Bmatrix}1\\0\end{Bmatrix} \tag{45}$$

The incident electric field from equations 39 can then be written as

$$\vec{E}_{inc} = E_o\vec{e}_2 e^{-i\vec{k}\cdot\vec{r}}$$

$$\vec{e}_2 e^{-i\vec{k}\cdot\vec{r}} = \sum_{n=1}^{\infty}\sum_{m=o}^{n}\left[a_{n,m}\vec{M}^{(1)}(n,m,o) + b_{n,m}\vec{N}^{(1)}(n,m,e)\right] \tag{46}$$

where

$$a_{n,m} = [2-\delta_{m,o}](-i)^{n+2}\,\frac{2n+1}{n(n+1)}\,m\,\frac{(n-m)!}{(n+m)!}\,\frac{P_n^m(\cos(\theta_1))}{\sin(\theta_1)}$$

$$b_{n,m} = [2-\delta_{m,o}](-i)^{n+1}\,\frac{2n+1}{n(n+1)}\,\frac{(n-m)!}{(n+m)!}\,\frac{dP_n^m(\cos(\theta_1))}{d\theta_1} \tag{47}$$

Setting $\vec{u} = \vec{e}_3$ we have another set of coefficients as

$$i\vec{e}_3 \cdot \vec{P}(n,m,{}^{e}_{o}) = -i\vec{e}_{\phi_1} \cdot \vec{P}(n,m,{}^{e}_{o}) = 0$$

$$\frac{1}{\sqrt{n(n+1)}}\,\vec{e}_3 \cdot \vec{C}(n,m,{}^{e}_{o}) = \frac{-1}{\sqrt{n(n+1)}}\,\vec{e}_{\phi_1} \cdot \vec{C}(n,m,{}^{e}_{o})$$

$$= \frac{1}{\sin(\theta_1)}\,\frac{1}{2n+1}\left[\frac{n-m+1}{n+1}\,P_{n+1}^m(\cos(\theta_1)) - \frac{n+m}{n}\,P_{n-1}^m(\cos(\theta_1))\right]\begin{Bmatrix}1\\0\end{Bmatrix}$$

$$= \frac{1}{n(n+1)}\,\frac{dP_n^m(\cos(\theta_1))}{d\theta_1}\begin{Bmatrix}1\\0\end{Bmatrix}$$

$$\frac{i}{\sqrt{n(n+1)}}\,\vec{e}_3 \cdot \vec{B}(n,m,{}^{e}_{o}) = \frac{-i}{\sqrt{n(n+1)}}\,\vec{e}_{\phi_1} \cdot \vec{B}(n,m,{}^{e}_{o}) \tag{48}$$

$$= \frac{-i}{\sin(\theta_1)}\,\frac{m}{n(n+1)}\,P_n^m(\cos(\theta_1))\begin{Bmatrix}0\\1\end{Bmatrix}$$

The incident magnetic field from equations 39 can then be written as

$$\vec{H}_{inc} = \frac{E_o}{Z}\,\vec{e}_3 e^{-i\vec{k}\cdot\vec{r}}$$

$$\vec{e}_3 e^{-i\vec{k}\cdot\vec{r}} = \sum_{n=1}^{\infty}\sum_{m=o}^{n}\left[ia_{n,m}\vec{N}^{(1)}(n,m,o) + ib_{n,m}\vec{M}^{(1)}(n,m,e)\right] \tag{49}$$

We then have the complete expansion of our incident wave.

Actually, with $\vec{e}_2 e^{-i\vec{k}\cdot\vec{r}}$ and $\vec{e}_3 e^{-i\vec{k}\cdot\vec{r}}$ expanded any polarization of the incident electric field (perpendicular to $\vec{k}$) can be written as a linear combination of these two plane waves. The associated incident magnetic field can be similarly written. Beginning with equations 44 we restricted $\phi_1 = 0$. However, if it is desired to have $\phi_1 \neq 0$ there are at least two approaches to generalize the present results. First, one can simply leave $\phi_1 \neq 0$ in calculating the coefficients as in equations 44 and 48; this will put terms like $\cos(m\phi_1)$ and $\sin(m\phi_1)$ in the coefficients. Or second, one can take advantage of the axial symmetry of the spherical coordinate system and consider $\phi - \phi_1$ as the azimuthal angle in the present results; in this case one just substitutes $\phi - \phi_1$ in place of ϕ in the $\vec{M}$ and $\vec{N}$ functions in equations 46 and 49. Which of these methods if used is a matter of convenience related to the problem at hand. As stated before we assume the spherical sensor in the present problem to have axial symmetry so that we use $\phi_1 = 0$ for convenience.

The expansion of $\vec{e}_1 e^{-i\vec{k}\cdot\vec{r}}$ would be another extension of the present results for cases where there were source currents in the incident wave such that the incident electric field had a non zero divergence. This, of course, would be accomplished by substituting $\vec{e}_1$ for $\vec{u}$ and obtaining a set of coefficients analogous to equations 44 or 48.

IV. Short Circuit Current

Having the incident plane wave, next consider the short circuit current from the sensor. For this calculation short circuit the gap in the sphere so that it looks like a complete perfectly conducting sphere with no gap. Then we consider the currents induced on the sphere by the incident plane wave. The incident plane wave is given by equations 46 and 49 in the previous section. Add to this a scattered wave of the form

$$\vec{E}_{sc} = E_o \sum_{n=1}^{\infty} \sum_{m=o}^{n} \left[c_{n,m} \vec{M}^{(4)}(n,m,o) + d_{n,m} \vec{N}^{(4)}(n,m,e) \right]$$

$$\vec{H}_{sc} = \frac{E_o}{Z} \sum_{n=1}^{\infty} \sum_{m=o}^{n} \left[ic_{n,m} \vec{N}^{(4)}(n,m,o) + id_{n,m} \vec{M}^{(4)}(n,m,e) \right] \qquad (50)$$

The fourth kind of spherical bessel functions are used to give an outward propagating wave; the $\vec{M}$ and $\vec{N}$ functions are chosen even or odd to match the ϕ dependence of those appearing in the expansion for the incident wave.

The boundary condition at r = a is that $E_\theta = E_\phi = 0$. From the spherical vector wave functions in equations 12 and 15 this requires

$$a_{n,m} j_n(ka) + c_{n,m} h_n^{(2)}(ka) = 0$$

$$b_{n,m} \frac{[kaj_n(ka)]'}{ka} + d_{n,m} \frac{\left[kah_n^{(2)}(ka)\right]'}{ka} = 0 \qquad (51)$$

giving

$$c_{n,m} = - \frac{j_n(ka)}{h_n^{(2)}(ka)} a_{n,m}$$

$$d_{n,m} = - \frac{[kaj_n(ka)]'}{\left[kah_n^{(2)}(ka)\right]'} b_{n,m} \qquad (52)$$

Note that the total field is

$$\vec{E} = \vec{E}_{inc} + \vec{E}_{sc} , \qquad \vec{H} = \vec{H}_{inc} + \vec{H}_{sc} \tag{53}$$

The surface current density $\vec{J}_s$ on the perfectly conducting spherical surface on r = a has θ and φ components which can be found from the magnetic field just outside the surface as

$$J_{s_\theta} = -H_\phi \Big|_{r=a+}$$

$$= \frac{E_o}{Z} \sum_{n=1}^{\infty} \sum_{m=o}^{n} \left\{ -ia_{n,m} \left\{ \frac{[kaj_n(ka)]'}{ka} - \frac{j_n(ka)}{h_n^{(2)}(ka)} \frac{\left[kah_n^{(2)}(ka)\right]'}{ka} \right\} \right.$$

$$\cdot \frac{P_n^m(\cos(\theta))}{\sin(\theta)} m \cos(m\phi)$$

$$\left. + ib_{n,m} \left\{ j_n(ka) - \frac{[kaj_n(ka)]'}{\left[kah_n^{(2)}(ka)\right]'} h_n^{(2)}(ka) \right\} \frac{dP_n^m(\cos(\theta))}{d\theta} \cos(m\phi) \right\} \tag{54}$$

$$J_{s_\phi} = H_\theta \Big|_{r=a+}$$

$$= \frac{E_o}{Z} \sum_{n=1}^{\infty} \sum_{m=o}^{n} \left\{ ia_{n,m} \left\{ \frac{[kaj_n(ka)]'}{ka} - \frac{j_n(ka)}{h_n^{(2)}(ka)} \frac{\left[kah_n^{(2)}(ka)\right]'}{ka} \right\} \right.$$

$$\cdot \frac{dP_n^m(\cos(\theta))}{d\theta} \sin(m\phi)$$

$$\left. - ib_{n,m} \left\{ j_n(ka) - \frac{[kaj_n(ka)]'}{\left[kah_n^{(2)}(ka)\right]'} h_n^{(2)}(ka) \right\} \frac{P_n^m(\cos(\theta))}{\sin(\theta)} m \sin(m\phi) \right\}$$

To simplify this we use a Wronskian relation[15] to obtain

$$h_n^{(2)}(ka)[kaj_n(ka)]' - j_n(ka)\left[kah_n^{(2)}(ka)\right]'$$

$$= \frac{-i}{ka}\left|kay_n(ka)[kaj_n(ka)]' - kaj_n(ka)[kay_n(ka)]'\right|$$

$$= \frac{i}{ka} \qquad (55)$$

Using this result in equations 54 gives

$$J_{s_\theta} = \frac{E_o}{Z}\sum_{n=1}^{\infty}\sum_{m=o}^{n}\left\{a_{n,m}\frac{1}{(ka)^2 h_n^{(2)}(ka)}\frac{P_n^m(\cos(\theta))}{\sin(\theta)} m \sin(m\phi)\right.$$

$$\left. + b_{n,m}\frac{1}{ka\left[kah_n^{(2)}(ka)\right]'}\frac{dP_n^m(\cos(\theta))}{d\theta}\cos(m\phi)\right\} \qquad (56)$$

$$J_{s_\phi} = \frac{E_o}{Z}\sum_{n=1}^{\infty}\sum_{m=o}^{n}\left\{-a_{n,m}\frac{1}{(ka)^2 h_n^{(2)}(ka)}\frac{dP_n^m(\cos(\theta))}{d\theta}\sin(m\phi)\right.$$

$$\left. - b_{n,m}\frac{1}{ka\left[kah_n^{(2)}(ka)\right]'}\frac{P_n^m(\cos(\theta))}{\sin(\theta)} m \sin(m\phi)\right\}$$

With surface current density on the sphere determined we can calculate the total current crossing a circle of constant θ on the spherical surface; this is

15. Ref. 6, eqn. 10.3.4.

$$I(\theta) \equiv a \sin(\theta) \int_0^{2\pi} J_{s_\theta} d\phi$$

$$= 2\pi a \sin(\theta) \frac{E_o}{Z} \sum_{n=1}^{\infty} b_{n,o} \frac{1}{ka\left[kah_n^{(2)}(ka)\right]'} \frac{dP_n^o(\cos(\theta))}{d\theta} \tag{57}$$

where

$$b_{n,o} = (-i)^{n+1} \frac{2n+1}{n(n+1)} \frac{dP_n^o(\cos(\theta_1))}{d\theta_1} \tag{58}$$

Rewriting the Legendre functions with the relation

$$\frac{dP_n^o(\cos(\theta))}{d\theta} = P_n^1(\cos(\theta)) \tag{59}$$

we then have

$$I(\theta) = 2\pi a \sin(\theta) \frac{E_o}{Z} \sum_{n=1}^{\infty} (-i)^{n+1} \frac{2n+1}{n(n+1)} \frac{1}{ka\left[kah_n^{(2)}(ka)\right]'}$$

$$\cdot P_n^1(\cos(\theta_1)) P_n^1(\cos(\theta)) \tag{60}$$

For small $|ka|$ we have for the spherical Hankel functions

$$h_n^{(2)}(ka) = i(2n-1)!!(ka)^{-n-1} + O\left((ka)^{-n}\right) \tag{61}$$

The double factorial function is defined by

$$\begin{aligned} (2n)!! &\equiv (2n)(2n-2) \cdots (4)(2) \qquad \text{(even)} \\ (2n-1)!! &\equiv (2n-1)(2n-3) \cdots (3)(1) \qquad \text{(odd)} \end{aligned} \tag{62}$$

with the conventions

$$0!! = 1 , \qquad (-1)!! = 1 \tag{63}$$

For small $|ka|$ the n = 1 term in equation 60 dominates and we have as $ka \to 0$

$$I(\theta) = 3\pi a \frac{E_o}{Z} (-ika) \sin(\theta_1)[\sin(\theta)]^2 + O\left((ka)^2\right)$$

$$= -3\pi a^2 E_o(\sigma + i\omega\varepsilon) \sin(\theta_1)[\sin(\theta)]^2 + O\left((ka)^2\right) \tag{64}$$

Thus for low frequencies the short circuit current is proportional to $(\sigma + i\omega\varepsilon)E_o \sin(\theta_1)$ which is the z component of the total current density. For the case that $\sigma = 0$ then the response is proportional to $i\omega\varepsilon E_o \sin(\theta_1)$ which (in the time domain) is just the z component of $\vec{D}$. Setting $\theta = \pi/2$ so that the position of the loop gap is on the equator of the sphere we have as $ka \to 0$

$$I(\pi/2) = -A_{eq}E_o(\sigma + i\omega\varepsilon) \sin(\theta_1) + O\left((ka)^2\right) \tag{65}$$

where the equivalent area of the sensor is

$$A_{eq} = 3\pi a^2 \tag{66}$$

or as a vector

$$\vec{A}_{eq} = 3\pi a^2 \vec{e}_z \tag{67}$$

so that we can write as $ka \to 0$

$$I(\pi/2) = -(\sigma + i\omega\varepsilon)\vec{E}_{inc}\Big|_{\vec{r}=\vec{0}} \cdot \vec{A}_{eq} + O\left((ka)^2\right) \tag{68}$$

For convenience we define a short circuit current transfer function as

$$T(\theta_1) \equiv I(\pi/2)[-A_{eq}E_o(\sigma + i\omega\varepsilon)]^{-1} \tag{69}$$

so that as $ka \to 0$ we have $T \to \sin(\theta_1)$ which is the ideal low-frequency angular dependence of the sensor. Then we have

$$T(\theta_1) = \frac{2}{3}\sum_{n=1}^{\infty}(-i)^n \frac{2n+1}{n(n+1)} \frac{1}{(ka)^2\left[kah_n^{(2)}(ka)\right]'} P_n^1(\cos(\theta_1))P_n^1(0) \quad (70)$$

Some special values for the Legendre functions are[16]

$$P_n^m(0) = \begin{cases} 0 \text{ for } n + m \text{ odd} \\ (-1)^{\frac{n+m}{2}} \frac{(n + m - 1)!!}{(n - m)!!} \text{ for } n + m \text{ even} \end{cases} \quad (71)$$

giving

$$T(\theta_1) = \sum_{n=1}^{\infty,2} \frac{2}{3} \frac{2n+1}{n(n+1)} \frac{n!!}{(n-1)!!} \frac{i}{(ka)^2\left[kah_n^{(2)}(ka)\right]'} P_n^1(\cos(\theta_1)) \quad (72)$$

where the second index above the summation sign is the increment which is added to the value of n to obtain the next value of n for the summation. Here only odd n result. For convenience define

$$T_n(\theta_1, \theta) \equiv (-i)^n \frac{2}{3} \frac{2n+1}{n(n+1)} \frac{1}{(ka)^2\left[kah_n^{(2)}(ka)\right]'} P_n^1(\cos(\theta_1))P_n^1(\theta) \quad (73)$$

For $\theta = \pi/2$ and odd n this is

$$T_n(\theta_1, \pi/2) = \frac{2}{3} \frac{2n+1}{n(n+1)} \frac{n!!}{(n-1)!!} \frac{i}{(ka)^2\left[kah_n^{(2)}(ka)\right]'} P_n^1(\cos(\theta_1)) \quad (74)$$

For our present case of interest just call this T_n so that the short circuit current transfer function can be written as

$$T(\theta_1) = \sum_{n=1}^{\infty,2} T_n \quad (75)$$

Note that as $ka \to 0$ we have $T \to T_1 \to \sin(\theta_1)$.

16. Ref. 7, p. 153.

The short circuit current transfer function is plotted in figure 4 as a function of ka with $\sigma = 0$. Note that we plot $T/\sin(\theta_1)$ for several values of θ_1. This is so that all the curves tend to one for low frequency and we can observe at what frequency (i.e. what ka) they start to spread from one another. For comparison T_1 from equation 74 is included. T_1 will be used later in calculating some of the sensor response functions. In figure 4 the magnitude and phase of $T/\sin(\theta_1)$ are plotted. For convenience the phase is plotted as arg(T) - ka which corresponds to multiplying T by e^{-ika}. This is the same type of display as used in reference 2. Note that the magnitude of $T/\sin(\theta_1)$ peaks up slightly at around ka = .7. Also, between ka = 1 and ka = 2 the response functions for various values of θ_1 begin to spread apart; some ka roughly between 1 and 2 can then be considered the upper frequency for which the sensor maintains a response proportional to $\sin(\theta_1)$ which can be considered the ideal angular dependence of the sensor. This range of ka is also where the frequency response (for the short circuit current) starts to fall off for higher frequencies.

$T_1/\sin(\theta_1)$ is a useful function to use for some of the later response function calculations because it is the first term in the expansion of $T/\sin(\theta_1)$ and because it has no dependence on θ_1. The Hankel function for n = 1 is just

$$h_1^{(2)}(ka) = \left[-\frac{1}{ka} + \frac{i}{(ka)^2}\right]e^{-ika} \tag{76}$$

Then T_1 is just

$$\frac{T_1}{\sin(\theta_1)} = \frac{-i}{(ka)^2\left[kah_n^{(2)}(ka)\right]'} = \frac{e^{ika}}{1 + ika - (ka)^2} \tag{77}$$

and we also have

$$\frac{T_1 e^{-ika}}{\sin(\theta_1)} = [1 + ika - (ka)^2]^{-1} \tag{78}$$

$T_1/\sin(\theta_1)$ has a peak magnitude of $2/\sqrt{3} \simeq 1.155$ occurring at $ka = 1/\sqrt{2} \simeq .707$.

V. Admittances

Now consider the admittances when the sensor is driven at the gap. As illustrated in figure 5 the loop gap is centered on $\theta = \pi/2$ and has an angular width of $2\psi_o$. There is a voltage V_{gap} uniformly distributed around the gap. Associated with V_{gap} there are three surface current densities which are parallel to $\hat{e}_\theta$. These are $J_{s_{ext}}$, $J_{s_{int}}$, and J_{s_c} and are associated respectively with fields external to the sphere, fields internal to the sphere, and currents into the cables or other transmission lines loading the gap. Taking the conventions for the directions of these currents as indicated in figure 5 we have three admittances to define, namely

$$Y_{int} \equiv 2\pi a \frac{J_{s_{int}}}{V_{gap}} , \quad Y_{ext} \equiv 2\pi a \frac{J_{s_{int}}}{V_{gap}} , \quad Y_c \equiv 2\pi a \frac{J_c}{V_{gap}} \tag{79}$$

In normalized form we also define

$$y_{int} \equiv ZY_{int} , \quad y_{ext} \equiv ZY_{ext} , \quad y_c \equiv ZY_c \tag{80}$$

For the numerical calculations we take $\sigma = 0$, as before. Also define a normalized cable conductance as

$$r_c \equiv \frac{1}{y_c} \equiv \frac{Z_c}{Z} \tag{81}$$

where Z_c is the net cable impedance (resistive) loading the gap. Since we have $\sigma = 0$ for the numerical calculations then $r_c \geq 0$ for such calculations and r_c is a constant which we can specify parametrically.

A. Boundary Conditions at Gap in Sphere

Here we use approximately the same quasi static approximation for the electric field distribution in the gap as was used in references 1 and 2. Defining

$$\psi \equiv \frac{\pi}{2} - \theta \tag{82}$$

we have

$$E_\theta\Big|_{r=a} = \frac{V_{gap}}{a\psi_o} f'_E\left(\frac{\psi}{\psi_o}\right) \tag{83}$$

with

$$f'_E(\zeta) = \begin{cases} \frac{1}{\pi}[1 - \zeta^2]^{-1/2} & \text{for } |\zeta| < 1 \\ 0 \quad \text{for } |\zeta| \geq 1 \end{cases} \tag{84}$$

This field distribution has the proper form of singularity at the edges of the gap, considering the assumption of a perfectly conducting spherical shell of zero thickness. The presence of cable connections across the gap will of course distort this field somewhat near the connections. However, of the various choices for the gap field one might choose the above choice seems to be a reasonable one. Note that we assume $\psi_o << 1$ for these calculations. Later we change to another field distribution f_E which closely approximates f'_E for small ψ. This other distribution will be more convenient for the evaluation of a certain integral.

B. Internal Admittance

To calculate the internal admittance we expand the fields inside the sphere in terms of the spherical vector wave functions. The boundary conditions at r = a are taken as independent of ϕ so that m = 0 for the wave functions. There are three non zero field components: E_r, $E\theta$, $H\phi$. The fields are finite at $\vec{r} = \vec{0}$ so that the spherical Bessel functions of the first kind are used. The fields are then expanded as

$$\vec{E}_{int} = E_1 \sum_{n=o}^{\infty} \alpha_n \vec{N}^{(1)}(n, 0, e)$$

$$\vec{H}_{int} = \frac{E_1}{Z} \sum_{n=o}^{\infty} i\alpha_n \vec{M}^{(1)}(n, 0, e) \tag{85}$$

where E_1 is some constant with dimensions volts/meter. The non zero components of the spherical vector wave functions for m = 0 from equations 12 and 15 are

$$M_{\phi}^{(\ell)}(n,0,e) = -f_n^{(\ell)}(kr)\frac{dP_n^o(\cos(\theta))}{d\theta} = -f_n^{(\ell)}(kr)P_n^1(\cos(\theta))$$

$$N_r^{(\ell)}(n,0,e) = n(n+1)\frac{f_n^{(\ell)}(kr)}{kr}P_n^o(\cos(\theta)) \tag{86}$$

$$N_{\theta}^{(\ell)}(n,0,e) = \frac{\left[krf_n^{(\ell)}(kr)\right]'}{kr}\frac{dP_n^o(\cos(\theta))}{d\theta} = \frac{\left[krf_n^{(\ell)}(kr)\right]'}{kr}P_n^1(\cos(\theta))$$

The boundary conditions for E_θ on r = a are given by equations 83 and 84. Writing out E_θ on r = a gives

$$E_\theta\Big|_{r=a} = E_1\sum_{n=o}^{\infty}\alpha_n\frac{[kaj_n(ka)]'}{ka}P_n^1(\cos(\theta)) \tag{87}$$

Multiplying both sides by $P_n^1(\cos(\theta))\sin(\theta)$, integrating over θ from 0 to π, and using the orthogonality of the Legendre functions gives[17]

$$\frac{V_{gap}}{a\psi_o}\int_o^{\pi} f_E'\left(\frac{\psi}{\psi_o}\right)P_n^1(\cos(\theta))\sin(\theta)d\theta = E_1\alpha_n\frac{[kaj_n(ka)]'}{ka}\frac{2n(n+1)}{2n+1} \tag{88}$$

For the integral we define a convenient term

$$\Lambda_n' \equiv \frac{1}{\psi_o}\int_o^{\pi} f_E'\left(\frac{\psi}{\psi_o}\right)P_n^1(\cos(\theta))\sin(\theta)d\theta$$

$$= \frac{1}{\psi_o}\int_{-\pi/2}^{\pi/2} f_E'\left(\frac{\psi}{\psi_o}\right)P_n^1(\sin(\psi))\cos(\psi)d\psi$$

$$= \frac{1}{\pi\psi_o}\int_{-\psi_o}^{\psi_o}\left[1-\left(\frac{\psi}{\psi_o}\right)^2\right]^{-1/2}P_n^1(\sin(\psi))[1-\sin^2(\psi)]^{1/2} \tag{89}$$

17. Ref. 6, eqn. 8.14.13.

Since we assume $\psi_o << 1$, then for $|\psi| \leq \psi_o$ we can use $\sin(\psi) \simeq \psi$ to write

$$\Lambda_n' \simeq \frac{1}{\pi\psi_o} \int_{-\psi_o}^{\psi_o} \left[1 - \left(\frac{\psi}{\psi_o}\right)^2\right]^{-1/2} [1 - \psi^2]^{1/2} P_n^1(\psi) d\psi \equiv \Lambda_n \qquad (90)$$

Then let $\zeta = \psi/\psi_o$ to give

$$\Lambda_n = \frac{1}{\pi} \int_{-1}^{1} [1 - \zeta^2]^{-1/2} \left[1 - \psi_o^2\zeta^2\right]^{1/2} P_n^1(\psi_o\zeta) d\zeta \qquad (91)$$

Since the form of f_E' is only approximate we take Λ_n instead of Λ_n' to calculate the coefficients. This integral is treated in appendix A. Using the approximation good for small ψ_o we then have for our coefficients

$$\alpha_n = \frac{V_{gap}}{aE_1} \frac{2n + 1}{2n(n + 1)} \frac{ka}{[kaj_n(ka)]'} \Lambda_n \qquad (92)$$

In obtaining the result of equation 91 for Λ_n the approximation $\sin(\psi) \simeq \psi$ was used for small ψ. This is equivalent to altering slightly the field distribution f_E' to one which we call f_E. To see this let $\psi_o\zeta = \sin(\psi)$ in equation 91 giving

$$\Lambda_n = \frac{1}{\pi\psi_o} \int_{-\arcsin(\psi_o)}^{\arcsin(\psi_o)} \left[1 - \left(\frac{\sin(\psi)}{\psi_o}\right)^2\right]^{-1/2} \cos(\psi) P_n^1(\sin(\psi)) \cos(\psi) d\psi$$

$$= \frac{1}{\psi_o} \int_{-\pi/2}^{\pi/2} f_E P_n^1(\sin(\psi)) \cos(\psi) d\psi \qquad (93)$$

where we have defined

$$f_E \equiv \begin{cases} \frac{1}{\pi}\left[1 - \left(\frac{\sin(\psi)}{\psi_o}\right)^2\right]^{-1/2} \cos(\psi) & \text{for } |\psi| < \arcsin(\psi_o) \\ 0 \quad \text{for } |\psi| \geq \arcsin(\psi_o) \end{cases} \qquad (94)$$

The voltage across the gap is given from equation 83 (except using f_E) by the integral

$$V_o = \frac{V_{gap}}{a\psi_o}\int_{-\pi/2}^{\pi/2} f_E a d\psi \tag{95}$$

Substituting from equation 94 and letting $\psi_o\zeta = \sin(\psi)$ we have

$$V_o = \frac{V_{gap}}{\pi}\int_{-1}^{1}[1 - \zeta^2]^{-1/2} d\zeta = V_{gap} \tag{96}$$

Thus this field distribution is still exactly consistent with V_{gap} as the gap voltage. The angular gap half width is $\arcsin(\psi_o)$ for this distribution and is very nearly ψ_o for small ψ. We thus take f_E as the field distribution across the gap instead of the simpler form given by f_E'.

The surface current density associated with the internal admittance is taken at $\theta = \pi/2$ for convenience so that we have

$$J_{s_{int}} \equiv -H_{int_\phi}\Big|_{\substack{r=a \\ \theta=\pi/2}} \tag{97}$$

From equations 85 we then have

$$J_{s_{int}} = \frac{E_1}{Z}\sum_{n=o}^{\infty} i\alpha_n j_n(ka) P_n^1(0) \tag{98}$$

From equation 71 we then have

$$J_{s_{int}} = \frac{E_1}{Z}\sum_{n=1}^{\infty,2} i(-1)^{\frac{n+1}{2}} \frac{n!!}{(n-1)!!}\alpha_n j_n(ka) \tag{99}$$

Note that only odd n contribute to this sum.

From equations 79 and 80 the normalized internal admittance is then

$$Y_{int} = \frac{2\pi aZ}{V_{gap}} J_{s_{int}} = \frac{2\pi aE_1}{V_{gap}} \sum_{n=1}^{\infty,2} iP_n^1(0)\alpha_n j_n(ka) \tag{100}$$

Substituting for α_n gives

$$Y_{int} = \sum_{n=1}^{\infty,2} i\pi \frac{2n+1}{n(n+1)} P_n^1(0)\Lambda_n \frac{kaj_n(ka)}{[kaj_n(ka)]'} \tag{101}$$

From appendix A, equation A21, we have

$$\Lambda_n = P_n^1(0)F\left(-\frac{n+1}{2}, \frac{n}{2}; 1; \psi_o^2\right) \tag{102}$$

where F is a hypergeometric function given by

$$F\left(-\frac{n+1}{2}, \frac{n}{2}; 1; \psi_o^2\right) = \sum_{q=o}^{\frac{n+1}{2}} \frac{\left(-\frac{n+1}{2}\right)_q \left(\frac{n}{2}\right)_q}{(q!)^2} \psi_o^{2q} \tag{103}$$

and where $(\alpha)_q$ is a Pochhammer symbol[18] defined by

$$(\alpha)_o \equiv 1$$

$$(\alpha)_q \equiv \alpha(\alpha+1)(\alpha+2) \cdots (\alpha+q-1) \quad \text{for } q = 1, 2, \cdots \tag{104}$$

Note that the series in equation 103 has only a finite number of terms giving a polynomial function of ψ_o. This is convenient for the numerical calculations. The normalized internal admittance can then be written as

$$Y_{int} = \sum_{n=1}^{\infty,2} i\pi \frac{2n+1}{n(n+1)} \left[P_n^1(0)\right]^2 F\left(-\frac{n+1}{2}, \frac{n}{2}; 1; \psi_o^2\right) \frac{kaj_n(ka)}{[kaj_n(ka)]'}$$

$$= \sum_{n=1}^{\infty,2} i\pi \frac{2n+1}{n(n+1)} \left[\frac{n!!}{(n-1)!!}\right]^2 F\left(-\frac{n+1}{2}, \frac{n}{2}; 1; \psi_o^2\right) \frac{kaj_n(ka)}{[kaj_n(ka)]'} \tag{105}$$

18. Ref. 6, eqn. 6.1.22.

The asymptotic properties of this series for large n are treated in appendix B.

The normalized internal admittance is plotted in figure 6 as a function of ka with $\sigma = 0$ for several values of ψ_o. Note that y_{int} has only an imaginary part. For convenience y_{int}/ka is plotted in figure 6; y_{int}/ka is an imaginary function for real ka which we are using. As $ka \to 0$ y_{int}/ka tends to a constant; the numerically determined coefficients are listed in table 1.

ψ_o	$\frac{y_{int}}{ika}$
.001	14.22
.01	9.62
.1	5.10

Table 1. Asymptotic form of y_{int} for small ka

As one would expect for small ka this admittance represents a capacitance. As ka is increased y_{int} has singularities corresponding to the zeros of $[kaj_n(ka)]'$. The first two singularities occur at $ka \simeq 2.744$ and $ka \simeq 4.973$.

C. External Admittance

The calculation of the external admittance follows the same development as the internal admittance. The fields outside the sphere are expanded as outward propagating waves in the forms

$$\vec{E}_{ext} = E_1 \sum_{n=o}^{\infty} \beta_n \vec{N}^{(4)}(n,0,e)$$

$$\vec{H}_{ext} = \frac{E_1}{Z} \sum_{n=o}^{\infty} i\beta_n \vec{M}^{(4)}(n,0,e) \qquad (106)$$

The only difference on the boundary r = a between these fields and those of equations 85 is the replacement of $j_n(ka)$ by $h_n^{(2)}(ka)$. Analogous to equation 92 we then have the expansion coefficients given by

$$\beta_n = \frac{V_{gap}}{aE_1} \frac{2n+1}{2n(n+1)} \frac{ka}{[kah_n^{(2)}(ka)]'} \Lambda_n \qquad (107)$$

where only odd n are of interest.

The surface current density associated with the external admittance is taken at $\theta = \pi/2$ giving

$$J_{s_{ext}} = H_{ext_\theta}\Big|_{\substack{r=a \\ \theta=\pi/2}}$$

$$= -\frac{E_1}{Z}\sum_{n=1}^{\infty,2} i\beta_n h_n^{(2)}(ka) P_n^1(0) \tag{108}$$

From equations 79 and 80 the normalized external admittance is then

$$y_{ext} = \frac{2\pi aZ}{V_{gap}} J_{s_{ext}} = \frac{2\pi aE_1}{V_{gap}} \sum_{n=1}^{\infty,2} (-i) P_n^1(0) \beta_n h_n^{(2)}(ka)$$

$$= \sum_{n=1}^{\infty,2} (-i)\pi \frac{2n+1}{n(n+1)} P_n^1(0) \Lambda_n \frac{kah_n^{(2)}(ka)}{\left[kah_n^{(2)}(ka)\right]'} \tag{109}$$

Or, substituting for Λ_n we have

$$y_{ext} = \sum_{n=1}^{\infty,2} (-i)\pi \frac{2n+1}{n(n+1)} \left[P_n^1(0)\right]^2 F\left(-\frac{n+1}{2}, \frac{n}{2}; 1; \psi_o^2\right) \frac{kah_n^{(2)}(ka)}{\left[kah_n^{(2)}(ka)\right]'}$$

$$= \sum_{n=1}^{\infty,2} (-i)\pi \frac{2n+1}{n(n+1)} \left[\frac{n!!}{(n-1)!!}\right]^2 F\left(-\frac{n+1}{2}, \frac{n}{2}; 1; \psi_o^2\right) \frac{kah_n^{(2)}(ka)}{\left[kah_n^{(2)}(ka)\right]'} \tag{110}$$

This series is very similar to the one in equation 105 and its asymptotic properties for large n are treated in appendix B.

The normalized external admittance is plotted in figure 7 as a function of ka with $\sigma = 0$ for several values of ψ_o. In this figure the real and imaginary parts of y_{ext} are plotted, again in the form y_{ext}/ka which tends to a constant for small ka; the numerically determined coefficients are listed in table 2.

ψ_o	$\frac{y_{ext}}{ika}$
.001	17.36
.01	12.75
.1	8.04

Table 2. Asymptotic form of y_{ext} for small ka

y_{ext} is also a capacitance for small ka. Note that as ka is increased y_{ext} does not have singularities as was the case with y_{int}.

VI. Frequency Response Characteristics

Now that we have the short circuit current and the admittances in suitably normalized forms we combine these results to calculate the frequency response characteristics. First define a response function including only the admittances as

$$R_y \equiv \frac{y_c}{y_{int} + y_{ext} + y_c} = [1 + r_c(y_{int} + y_{ext})]^{-1} \qquad (111)$$

This is plotted as a function of ka in figures 8 and 9 for two values of ψ_o (.01 and .1) with $\sigma = 0$. For each graph several values of r_c are used. Note for $r_c > 0$ that R_y has zeros at the singularities of y_{int}. As one would expect decreasing r_c maintains R_y as a flat response characteristic out to larger values of ka which represents higher frequency response.

Including the short circuit current transfer function from equation 75 we have the response function

$$R(\theta_1) \equiv \frac{T(\theta_1)}{\sin(\theta_1)} R_y = \frac{T(\theta_1)}{\sin(\theta_1)}[1 + r_c(y_{int} + y_{ext})]^{-1} \qquad (112)$$

Another convenient, but somewhat artificial response function is given by

$$R_1 \equiv \frac{T_1}{\sin(\theta_1)} R_y = \frac{T_1}{\sin(\theta_1)}[1 + r_c(y_{int} + y_{ext})]^{-1} \qquad (113)$$

This last response function uses only the first term in the expansion for $T(\theta_1)$ and is independent of θ_1.

In figures 10 and 11 we have R_1 plotted as a function of ka for two values of ψ_o (.01 and .1) and several values of r_c. Note that the factor $T_1/\sin(\theta_1)$ peaks up the frequency response in the vicinity of ka = 1, partially compensating for the rolloff with frequency associated with R_y.

Based on R_1 we define an upper frequency response as the minimum value of ka for which

$$|R_1| = \frac{1}{\sqrt{2}} \qquad (114)$$

This value of ka is plotted as a function of r_c in figure 12 for two values of ψ_o. Frequency response is increased by increasing ψ_o and by decreasing r_c. It may not be desirable to decrease r_c too far because as $r_c \to 0$ no power is delivered to the output.

In figures 13 and 14 we have plotted R as a function of ka with $\sigma = 0$ for various values of θ_1 with $\psi_o = .1$ for two specific values of r_c. These two values are $r_c \simeq .1327$ and $r_c \simeq .2654$ which correspond to $Z_c = 50\ \Omega$ and $Z_c = 100\ \Omega$ respectively if the media inside and outside the sphere are assumed to have the same constitutive parameters as free space so that the wave impedance is

$$Z = Z_o \simeq 376.7\ \Omega \tag{115}$$

Using R_1 as an average of R to remove the dependence on θ_1, the frequency responses for these two cases as defined by equation 114 are given by ka $\simeq .60$ and ka $\simeq .30$ for $Z_c = 50\ \Omega$ and $Z_c = 100\ \Omega$ respectively.

VII. Summary

In this note we have developed frequency and angular response curves for the hollow spherical dipole with a uniformly resistively loaded equatorial slot. For these calculations the media inside and outside the sphere were assumed to have the same permittivity and permeability and zero conductivity. For low frequencies the response of this kind of sensor is proportional to one component of the displacement current density (which is also called the time rate of change of the displacement vector).

As an extension of the present calculations one might consider the case that the external medium was a linear conducting medium. In this case if the resistance due to the signal cable loading (Z_c) were small compared to the resistance loading due to the conducting medium, then for low frequencies this sensor would have a response proportional to the total current density (conduction plus displacement) in the external medium.

Perhaps the design considered in this note can be extended to the case of several slots around the sphere at different values of θ. This would be a multi-gap spherical dipole analogous to the multi-gap cylindrical loop. Another extension of the present calculations would be to loops with spherical geometries. Perhaps some of these and related topics can be considered in future notes.

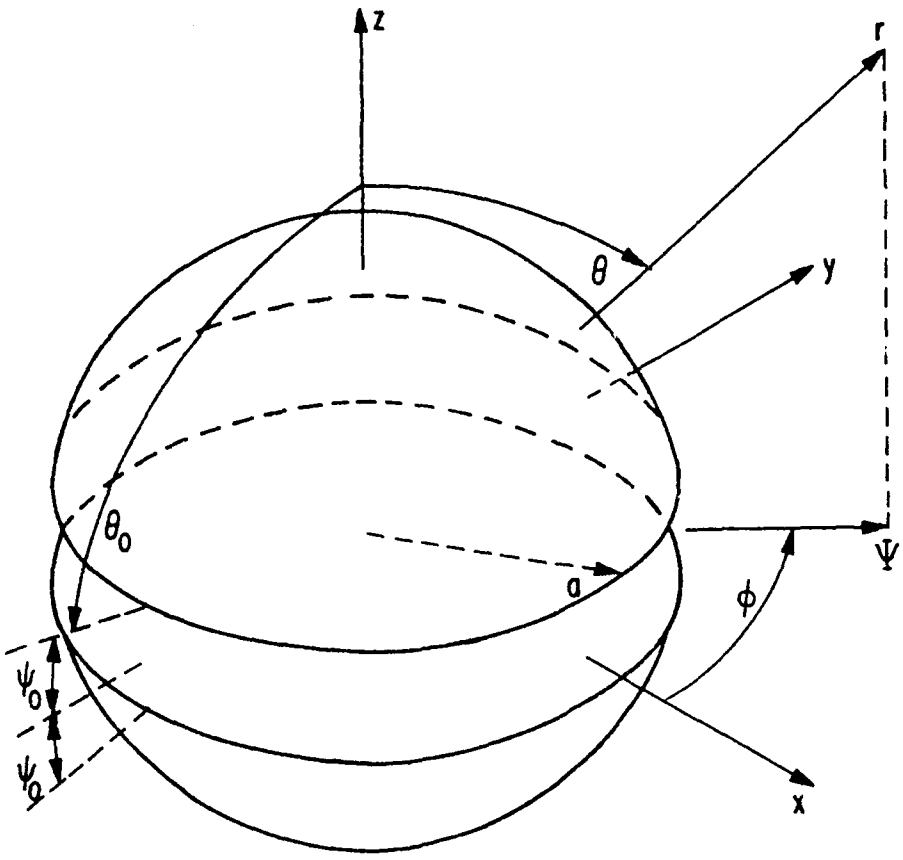

FIGURE 1. SINGLE-GAP HOLLOW SPHERICAL DIPOLE

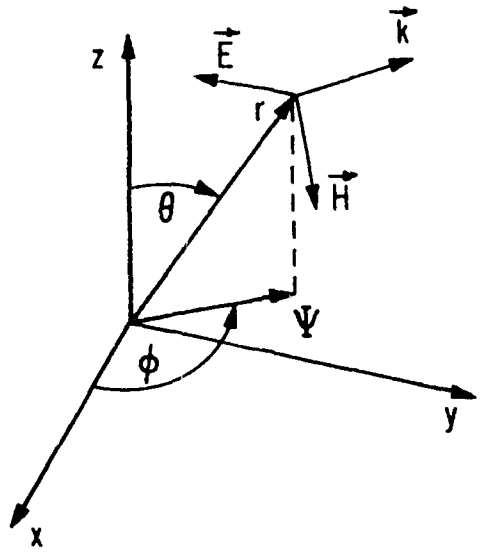

A. PLANE WAVE WITH FIXED POLARIZATION

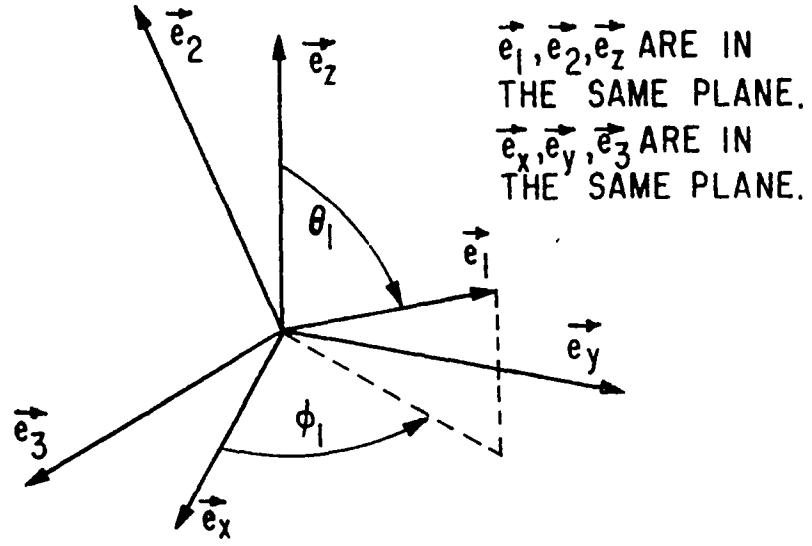

B. UNIT VECTORS FOR PLANE WAVES

FIGURE 2. VECTOR PLANE WAVES IN SPHERICAL COORDINATES

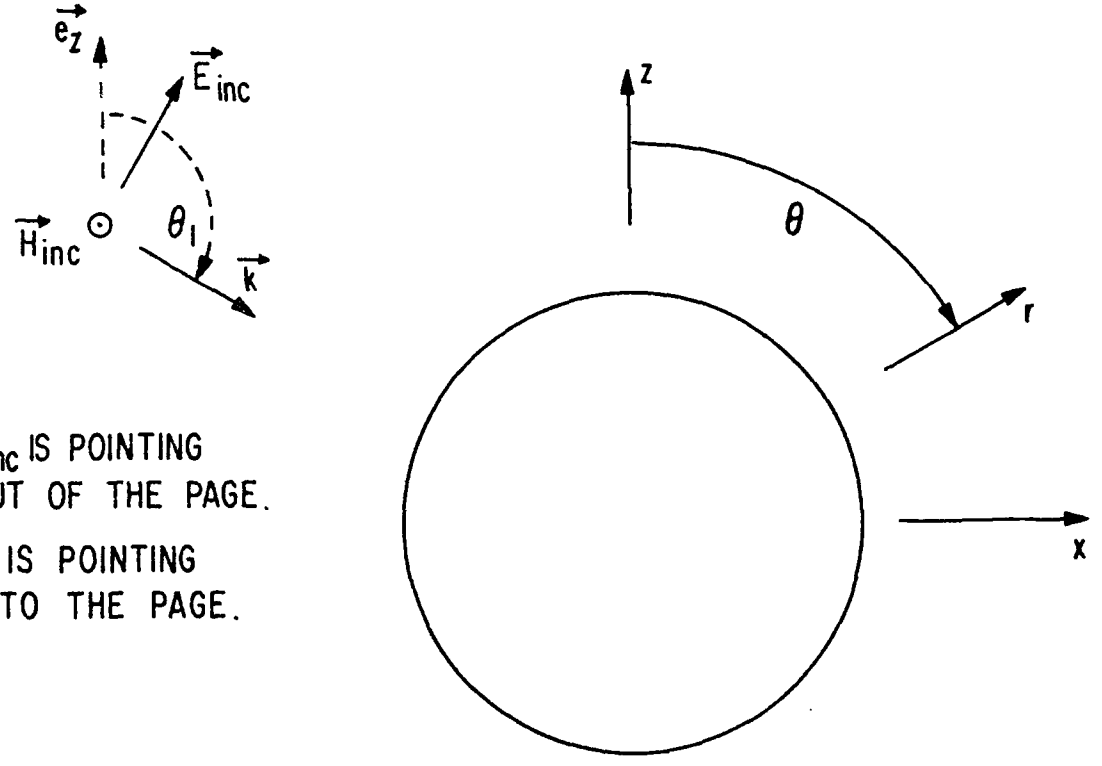

$\vec{H}_{inc}$ IS POINTING OUT OF THE PAGE.

y IS POINTING INTO THE PAGE.

FIGURE 3. PLANE WAVE INCIDENT ON SPHERE: CROSS-SECTION VIEW WITH $\phi_1 = 0$

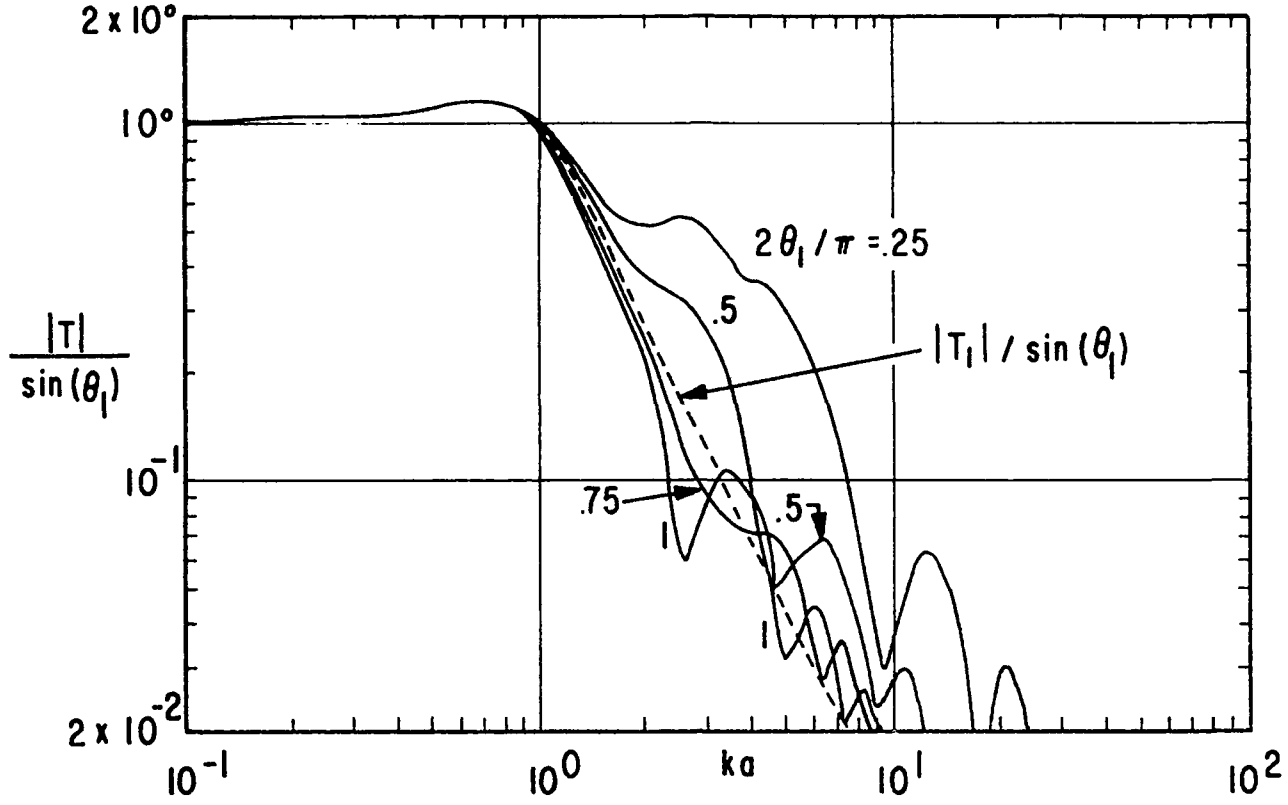

A. MAGNITUDE OF T/sin(θ_1) WITH θ_1 AS A PARAMETER

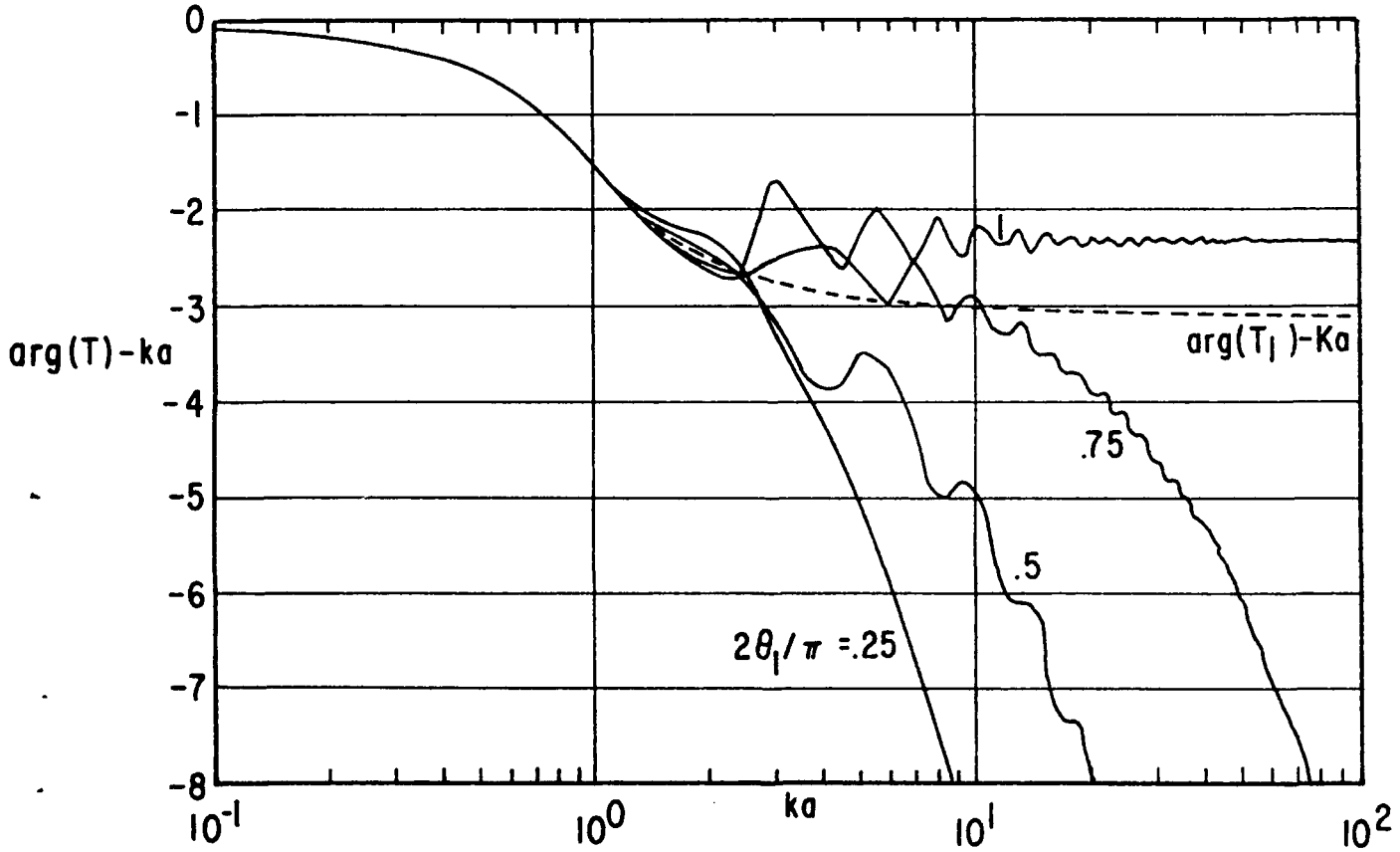

B. PHASE OF T WITH θ_1 AS A PARAMETER

FIGURE 4. SHORT CIRCUIT CURRENT TRANSFER FUNCTION

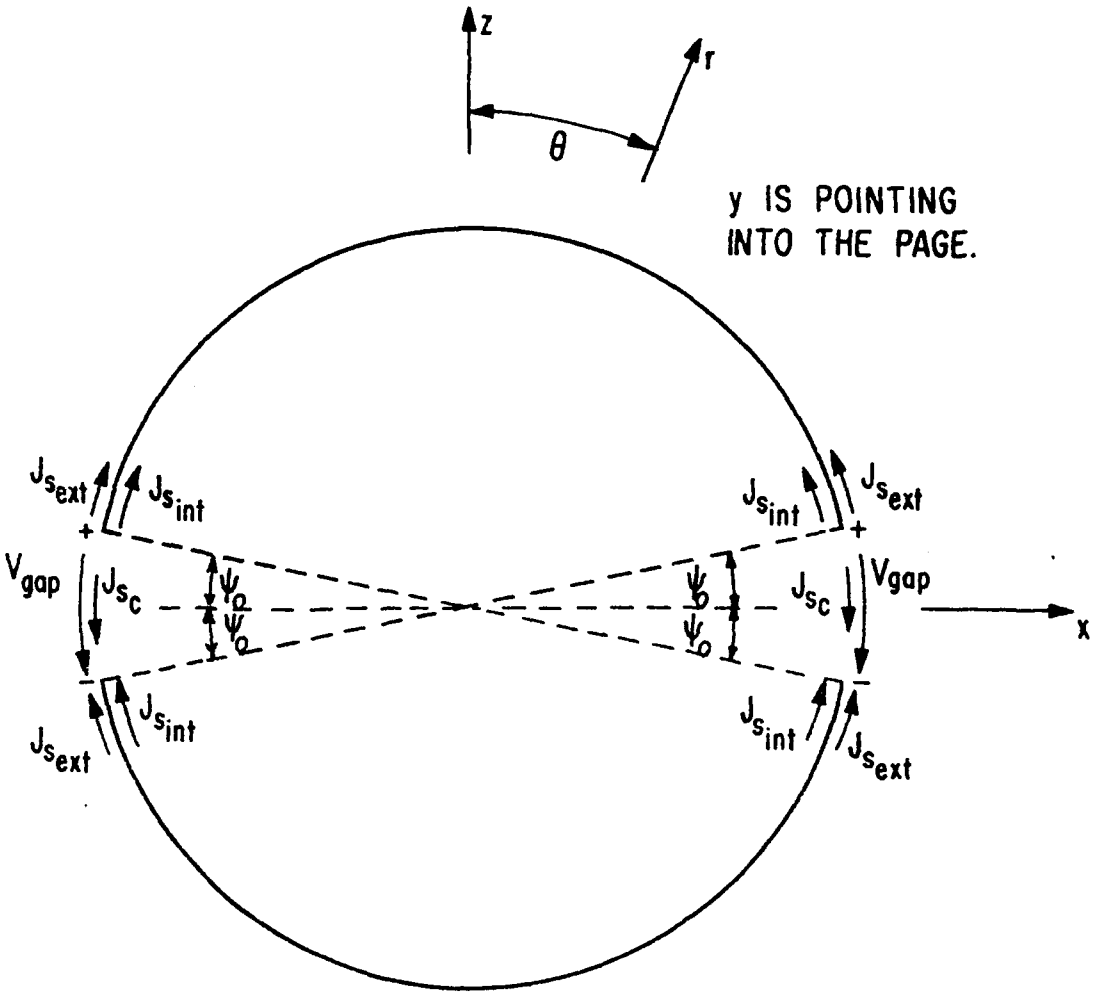

FIGURE 5. CURRENTS ON SPHERE FOR ADMITTANCES: CROSS SECTION VIEW

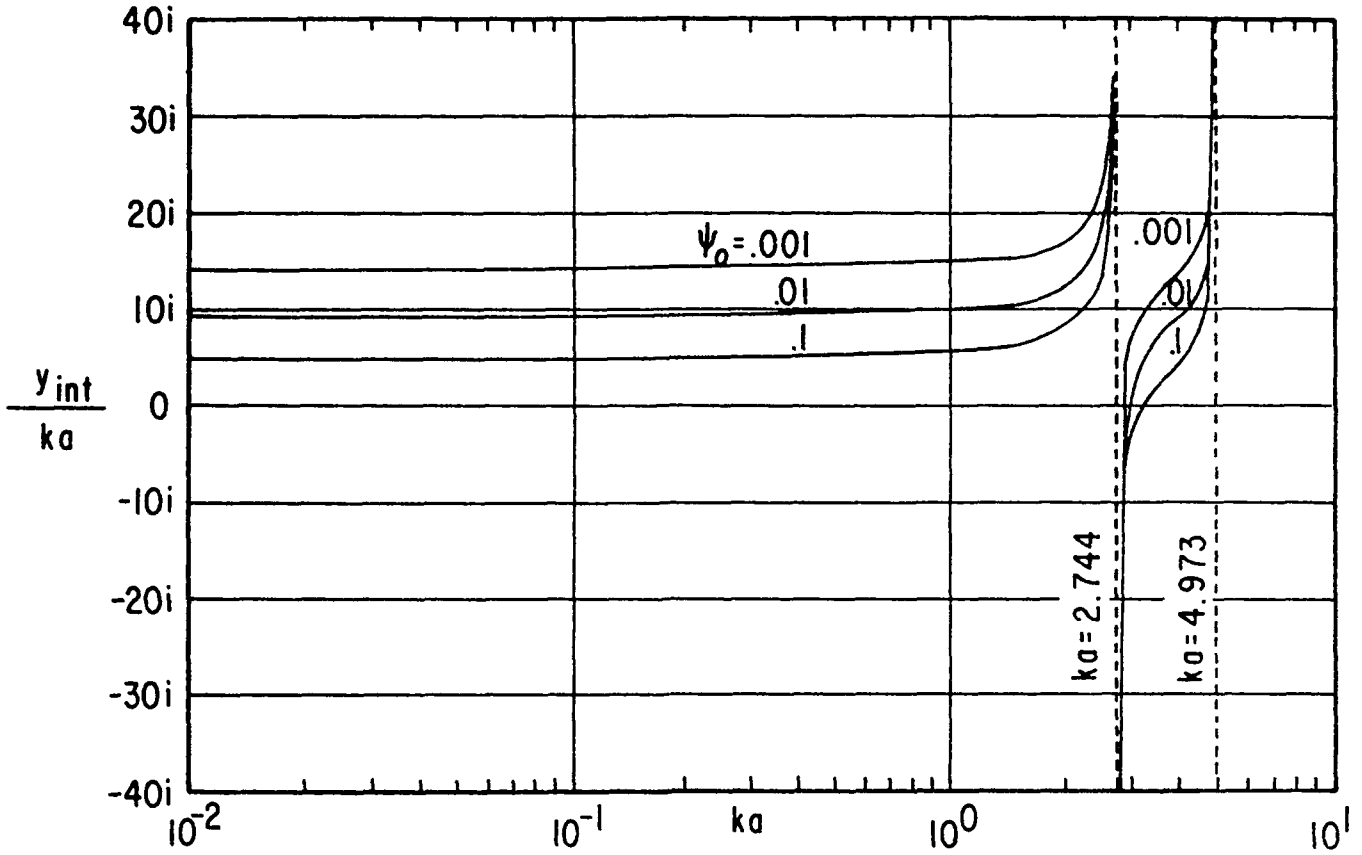

A. y_{int}/ka WITH ψ_0 AS A PARAMETER

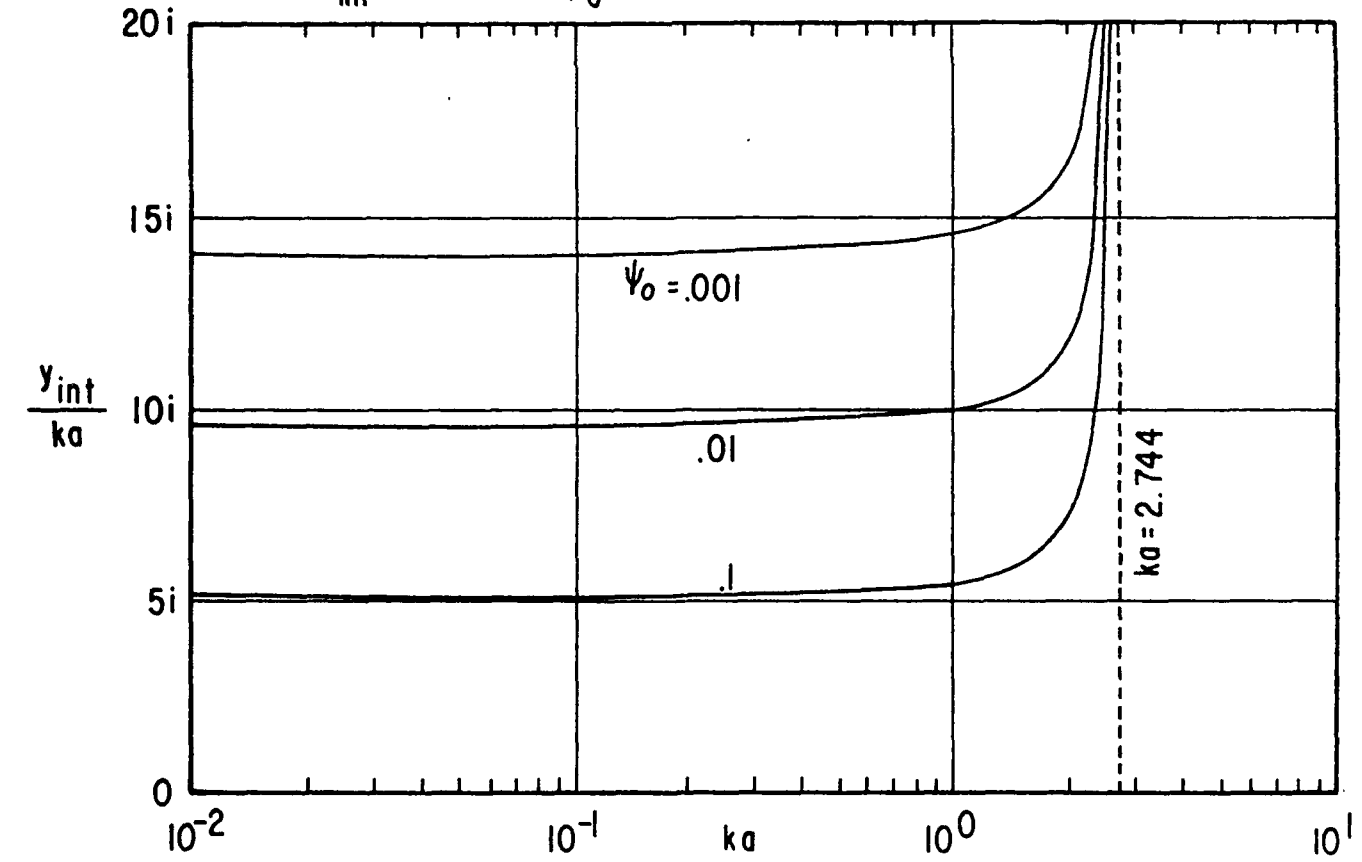

B. SCALE OF A EXPANDED

FIGURE 6. NORMALIZED INTERNAL ADMITTANCE

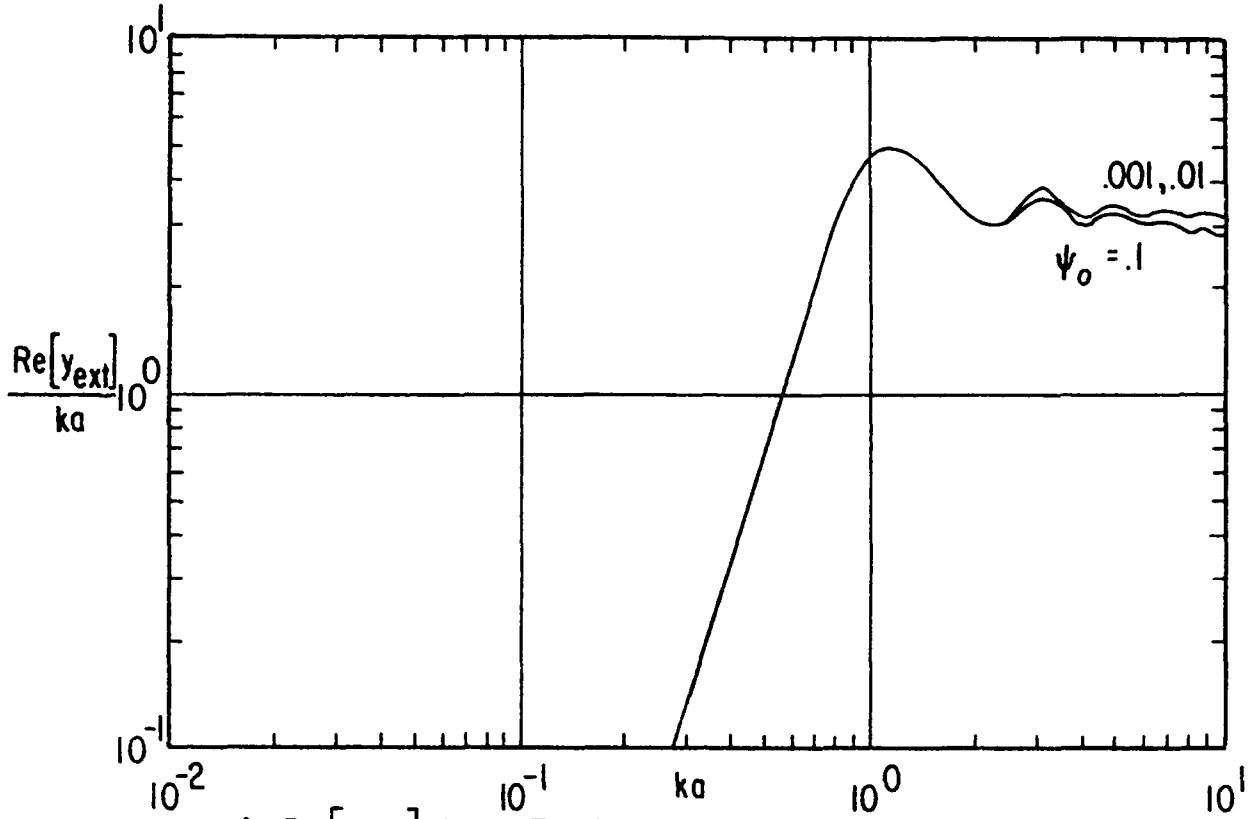

A. $Re\left[y_{ext}\right]/ka$ WITH ψ_o AS A PARAMETER

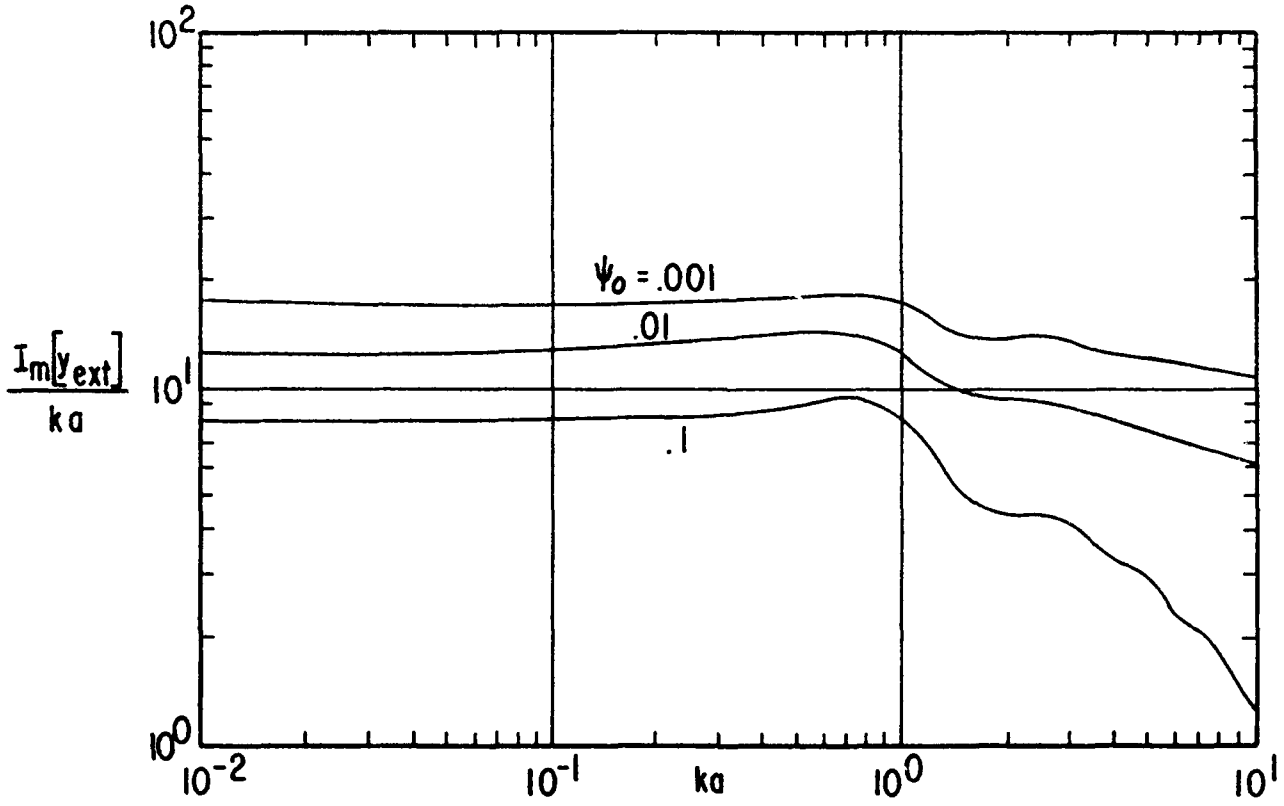

B. $I_m\left[y_{ext}\right]/ka$ WITH ψ_o AS A PARAMETER

FIGURE 7. NORMALIZED EXTERNAL ADMITTANCE

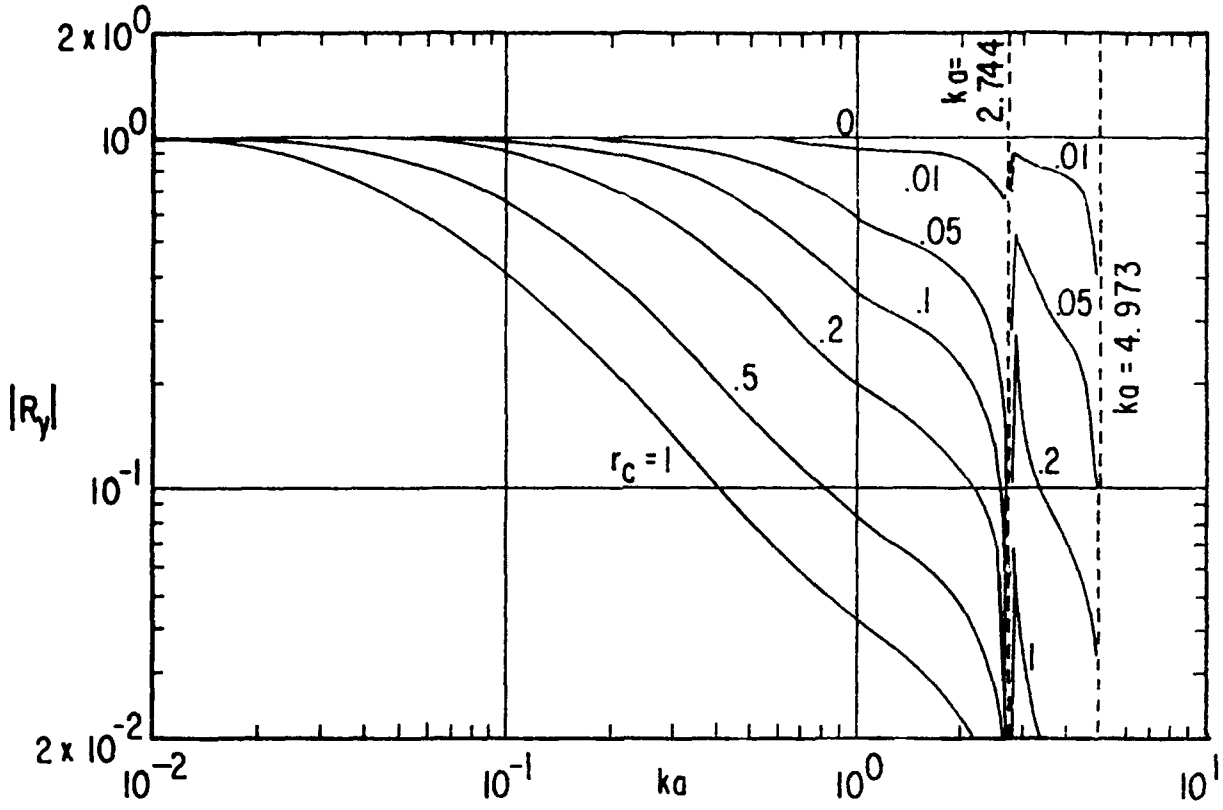

A. MAGNITUDE OF R_y WITH r_c AS A PARAMETER

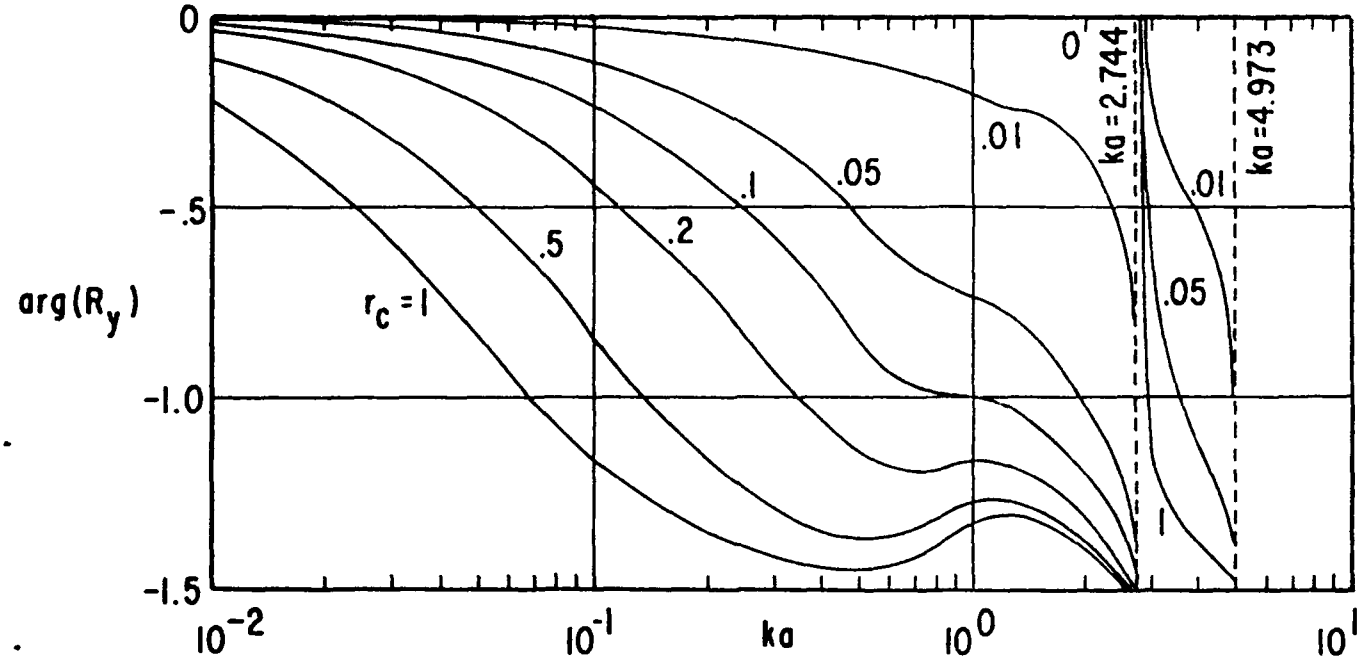

B. PHASE OF R_y WITH r_c AS A PARAMETER

FIGURE 8. EFFECT OF ADMITTANCES ON RESPONSE: $\psi_o = .01$

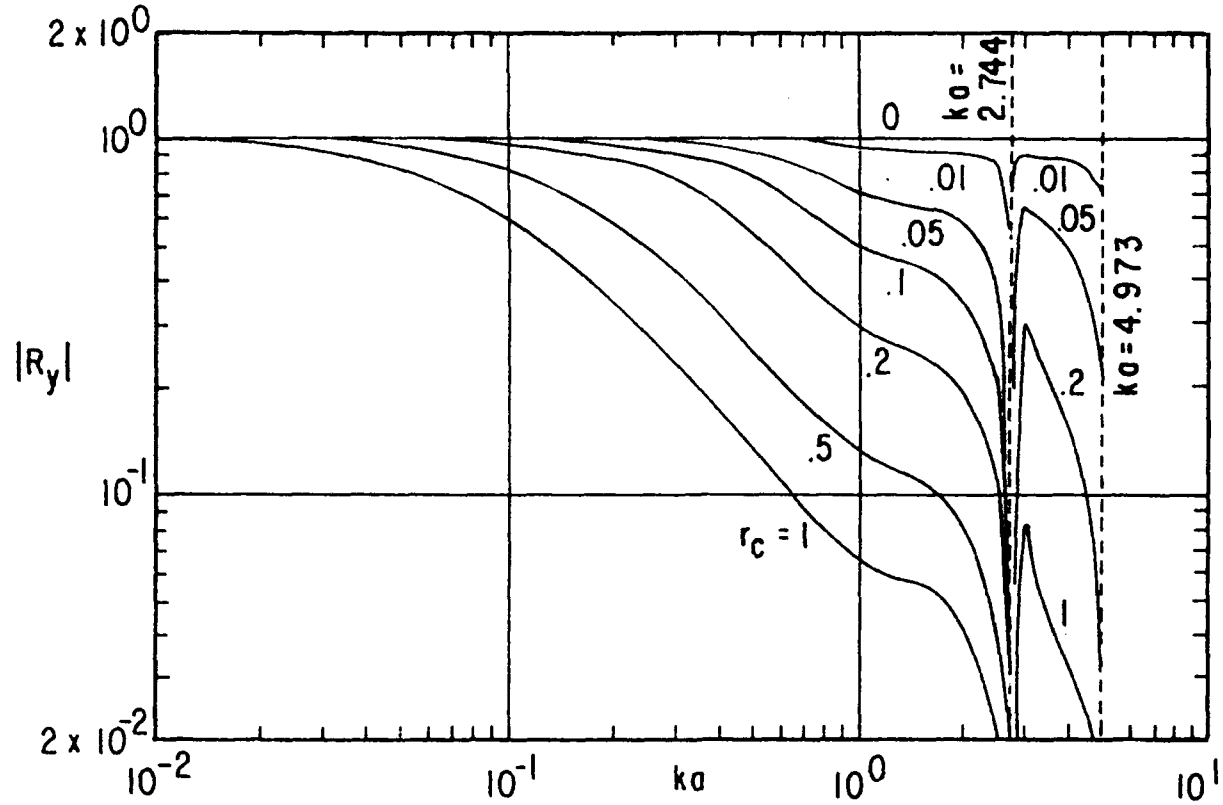

A. MAGNITUDE OF R_y WITH r_c AS A PARAMETER

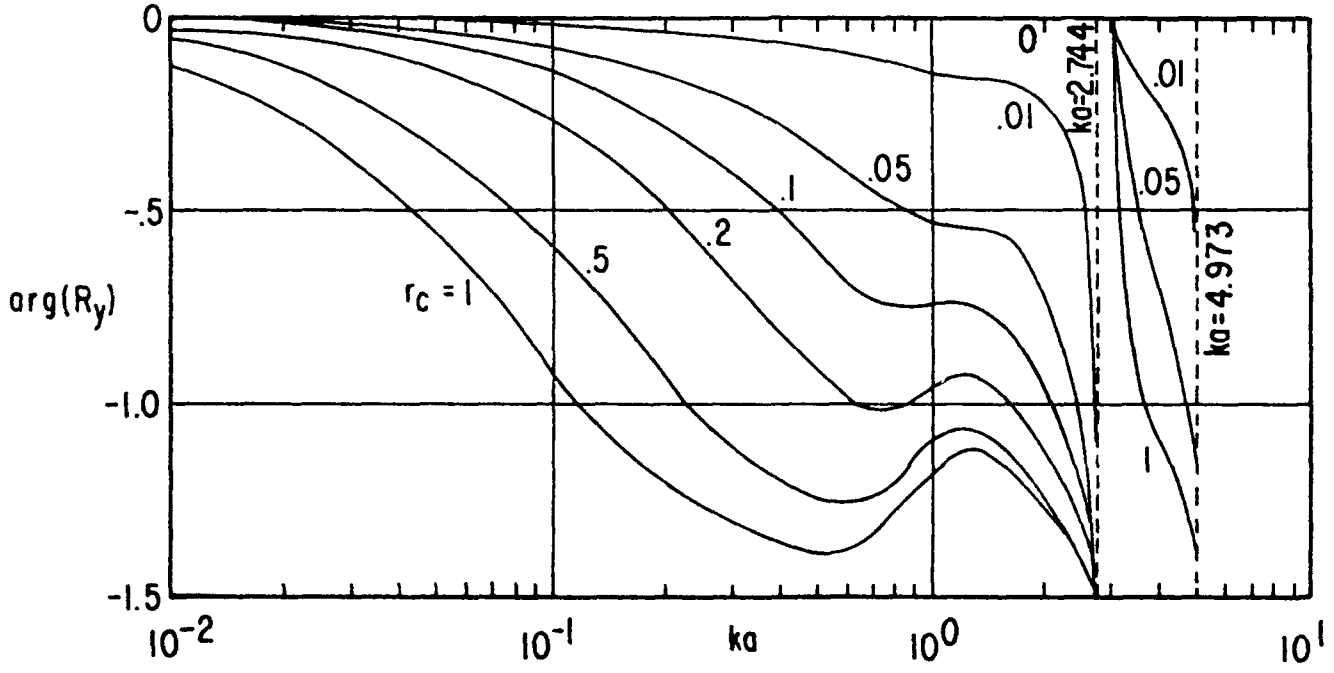

B. PHASE OF R_y WITH r_c AS A PARAMETER

FIGURE 9. EFFECT OF ADMITTANCES ON RESPONSE: $\psi_o = .1$

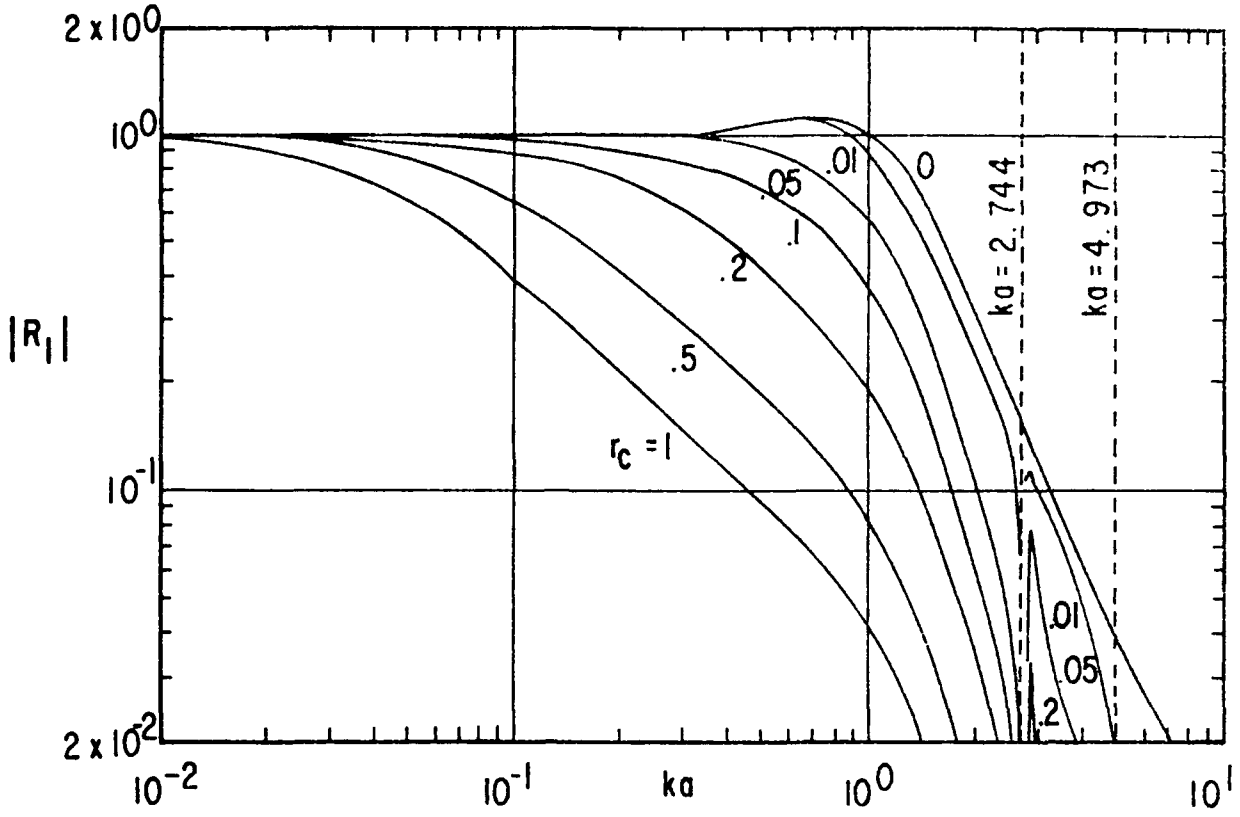

A. MAGNITUDE OF R_1 WITH r_c AS A PARAMETER

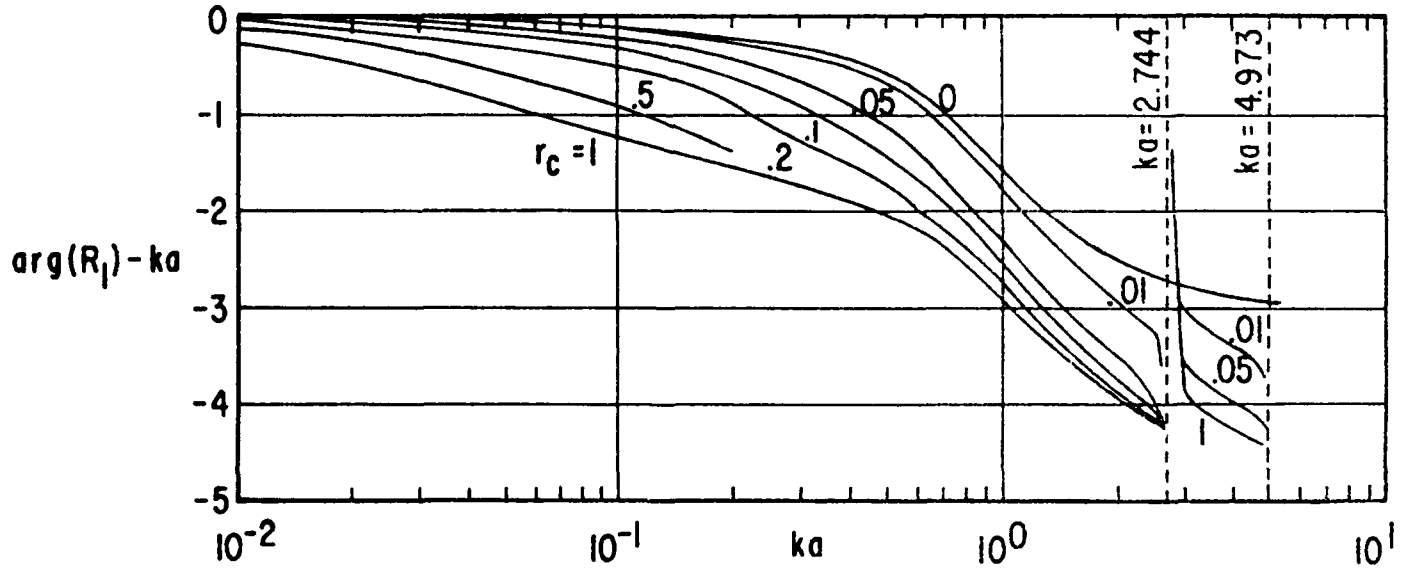

B. PHASE OF R_1 WITH r_c AS A PARAMETER

FIGURE 10. ARTIFICIAL RESPONSE CHARACTERISTS: $\psi_0 = .01$

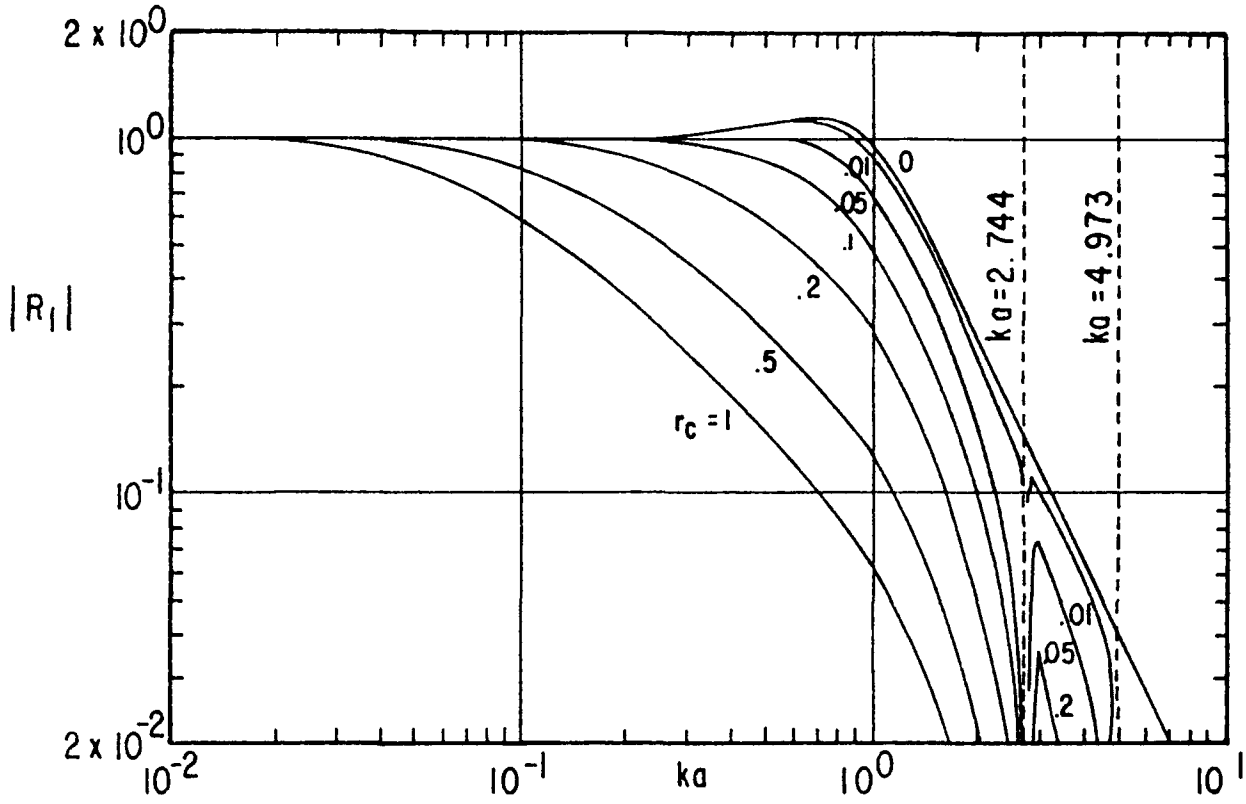

A. MAGNITUDE OF R_1 WITH r_c AS A PARAMETER

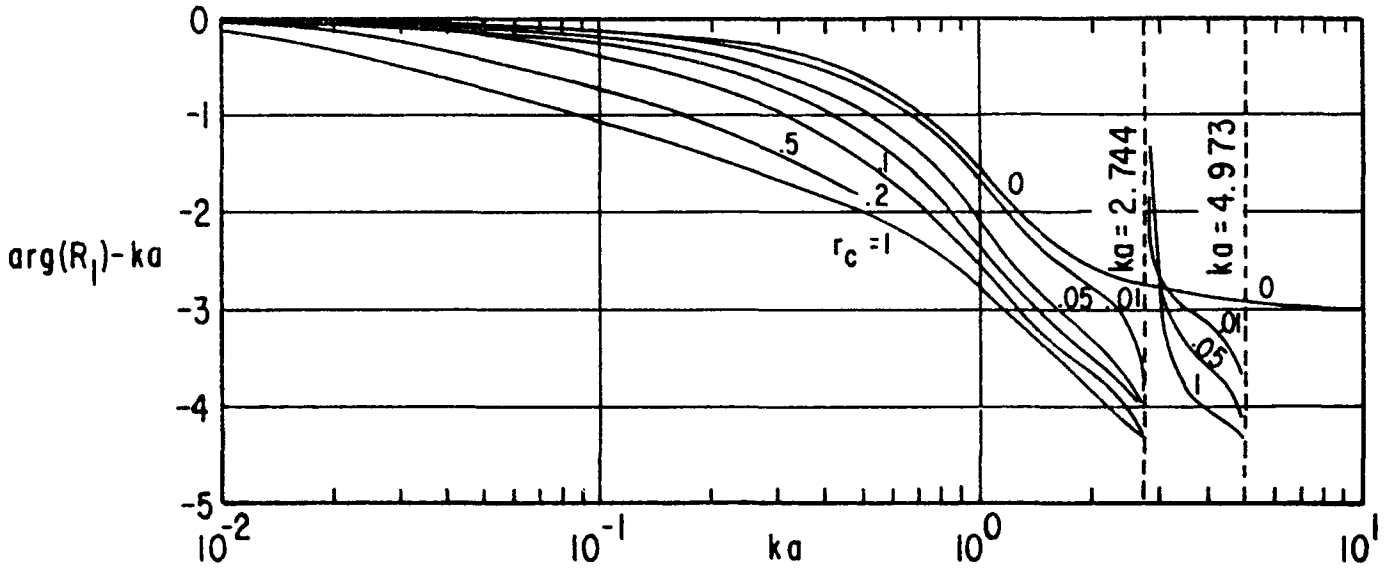

B. PHASE OF R_1 WITH r_c AS A PARAMETER

FIGURE 11. ARTIFICIAL RESPONSE CHARACTERISTICS: $\psi_0 = .1$

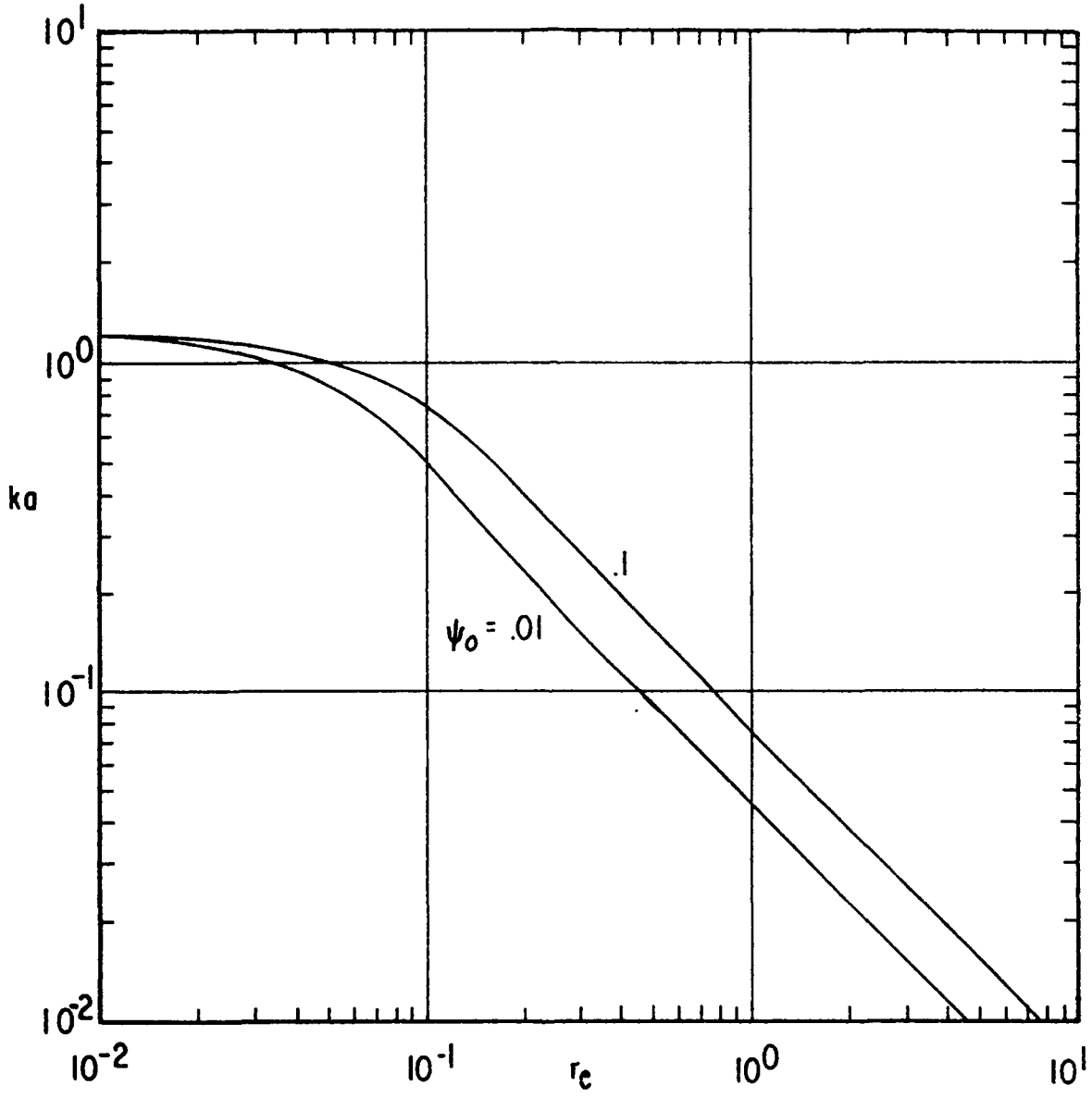

FIGURE 12. DEPENDENCE OF FREQUENCY RESPONSE ON CABLE IMPEDANCE WITH ψ_o AS A PARAMETER: $|R_1| = 1/\sqrt{2}$

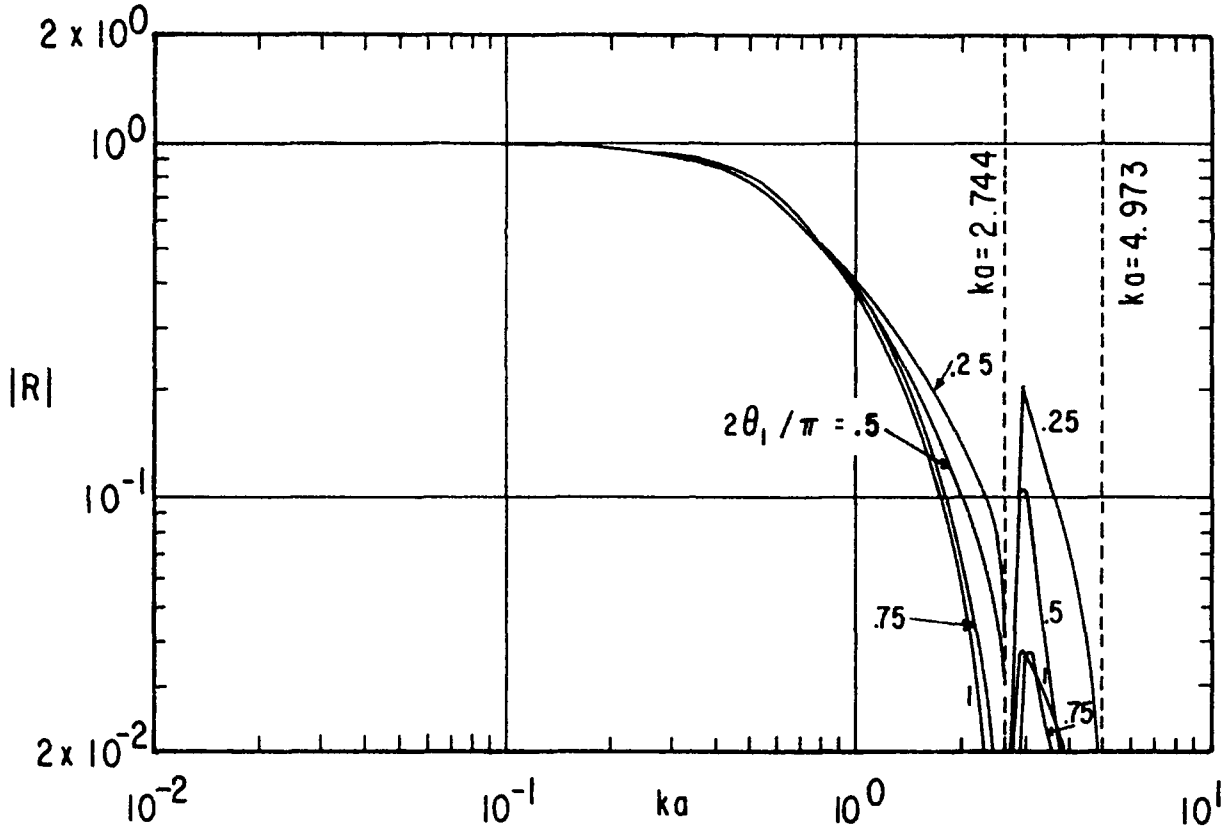

A. MAGNITUDE OF R WITH θ_1 AS A PARAMETER

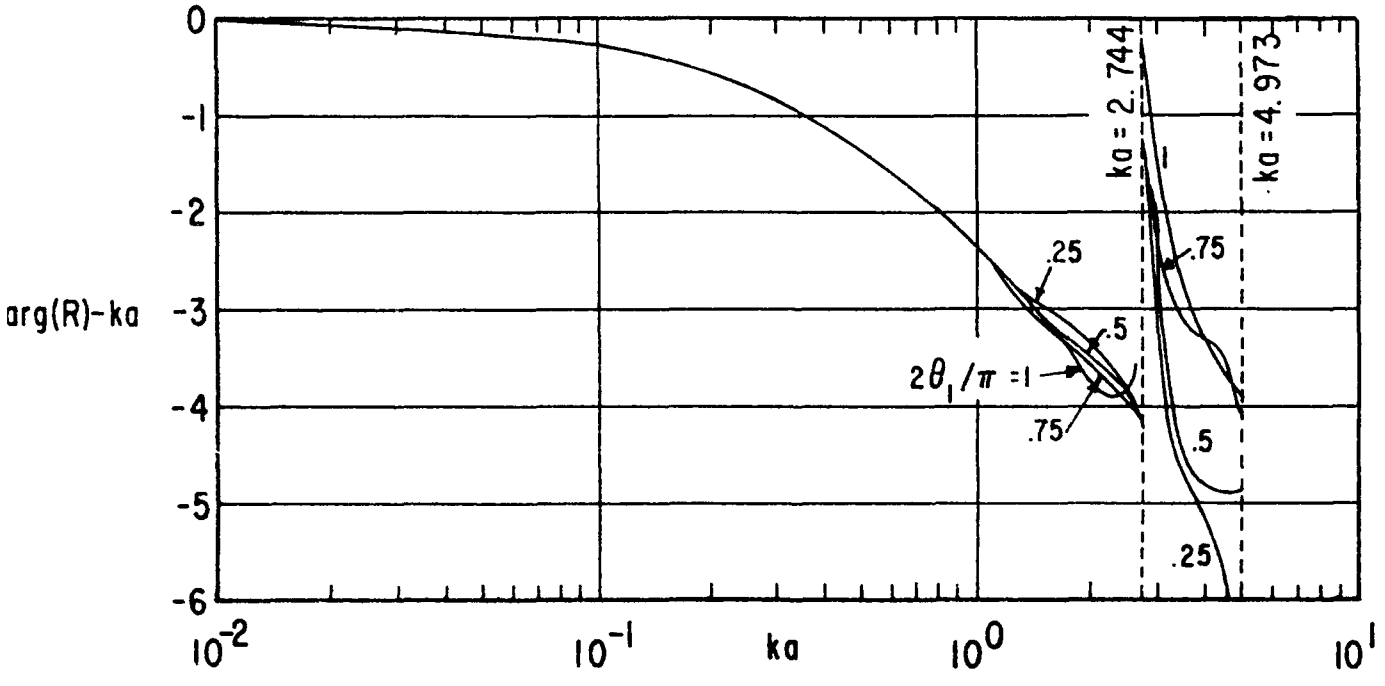

B. PHASE OF R WITH θ_1 AS A PARAMETER

FIGURE 13. RESPONSE CHARACTERISTICS: $\psi_0 = .1$, $r_c = 50\Omega / Z_0 \simeq .1327$

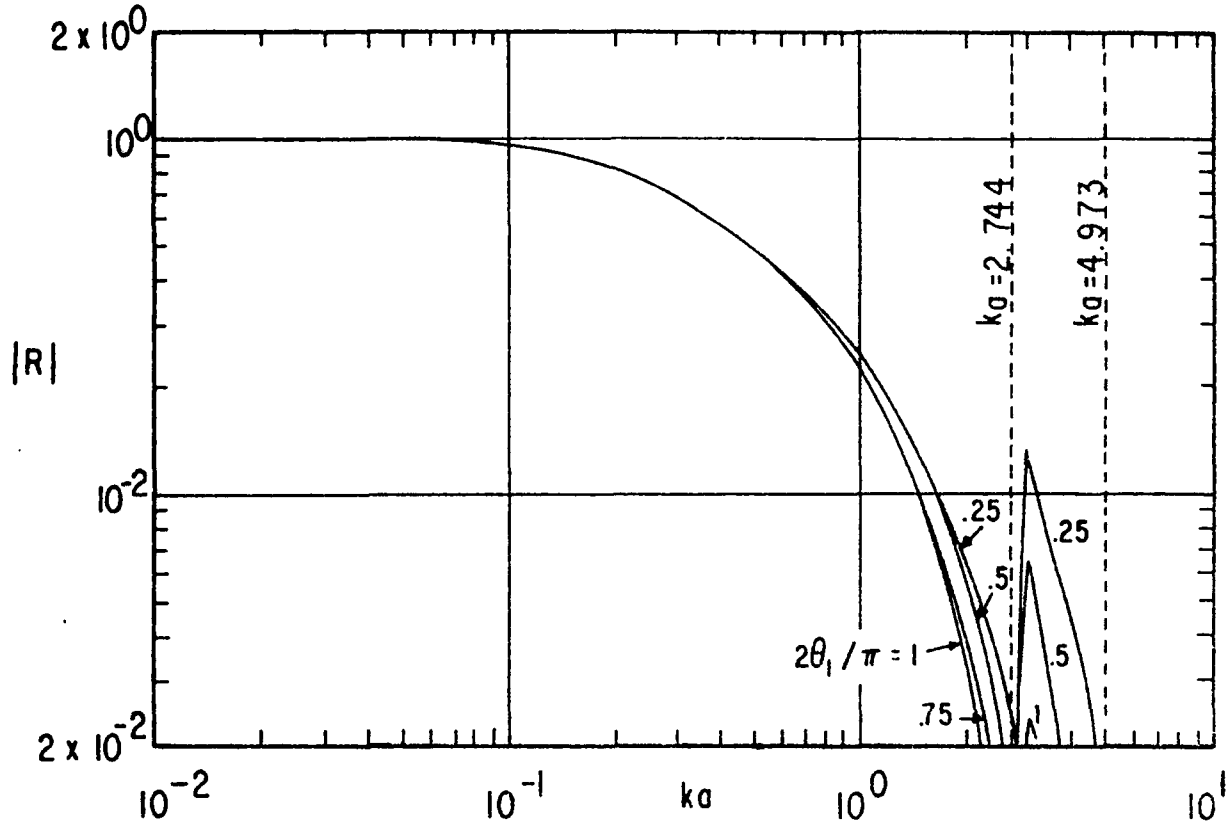

A. MAGNITUDE OF R WITH θ_1 AS A PARAMETER

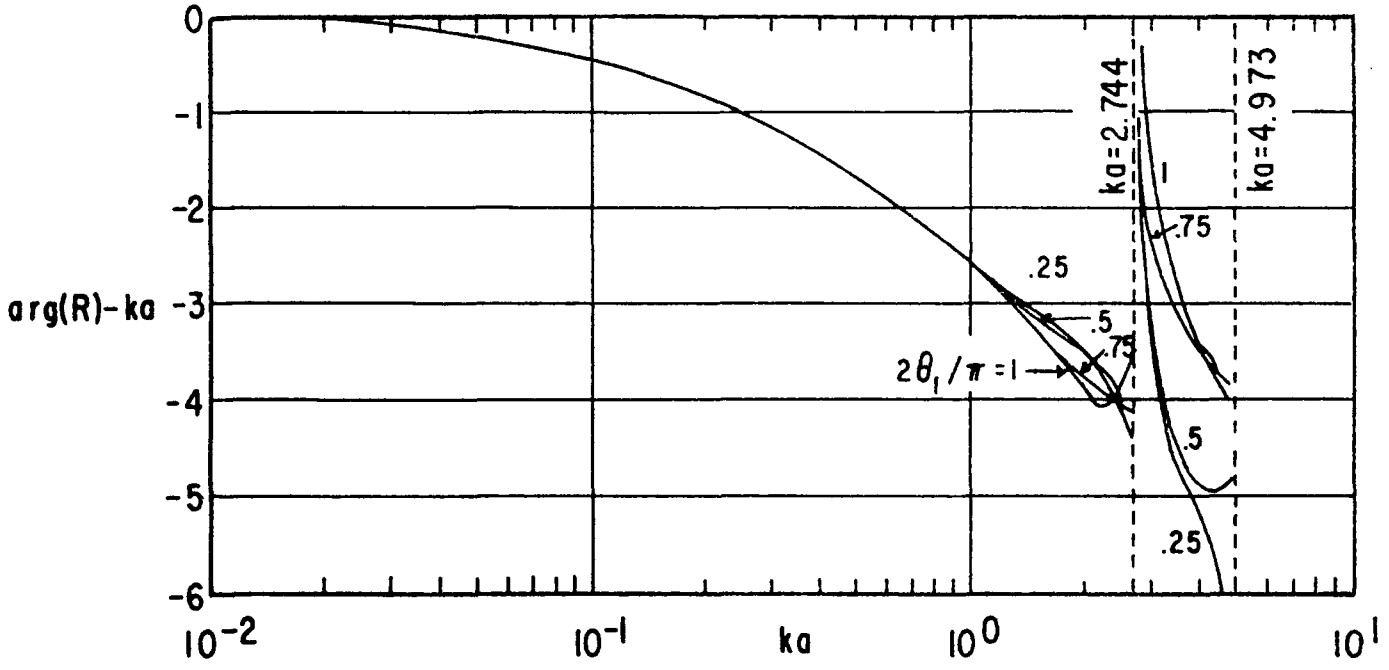

B. PHASE OF R WITH θ_1 AS A PARAMETER

FIGURE 14. RESPONSE CHARACTERISTICS: $\psi_0 = .1$, $r_c = 100\Omega / Z_0 \cong .2654$

Appendix A: Calculation of Λ_n

In equation 91 we have a function which is expressed as an integral given by

$$\Lambda_n = \frac{1}{\pi}\int_{-1}^{1} [1 - \zeta^2]^{-1/2}\left[1 - \psi_o^2\zeta^2\right]^{1/2} P_n^1(\psi_o\zeta)d\zeta \qquad \text{(A1)}$$

This function appears in the coefficients of the field expansions used to calculate the internal and external admittances of the sensor. The purpose of this appendix is to calculate this integral.

Define

$$\Xi_1 = \int_{-1}^{1} [1 - \zeta^2]^{\lambda-1}\left[1 - \psi_o^2\zeta^2\right]^{\mu/2} P_\nu^\mu(\psi_o\zeta)d\zeta \qquad \text{(A2)}$$

Rearrange this as

$$\Xi_1 = \int_{-1}^{0} [1 - \zeta^2]^{\lambda-1}\left[1 - \psi_o^2\zeta^2\right]^{\mu/2} P_\nu^\mu(\psi_o\zeta)d\zeta$$

$$+ \int_{o}^{1} [1 - \zeta^2]^{\lambda-1}\left[1 - \psi_o^2\zeta^2\right]^{\mu/2} P_\nu^\mu(\psi_o\zeta)d\zeta$$

$$= \int_{o}^{1} [1 - \zeta^2]^{\lambda-1}\left[1 - \psi_o^2\zeta^2\right]^{\mu/2} P_\nu^\mu(-\psi_o\zeta)d\zeta$$

$$+ \int_{o}^{1} [1 - \zeta^2]^{\lambda-1}\left[1 - \psi_o^2\zeta^2\right]^{\mu/2} P_\nu^\mu(\psi_o\zeta)d\zeta \qquad \text{(A3)}$$

giving

$$\Xi_1 = \int_0^1 [1 - \zeta^2]^{\lambda-1}\left[1 - \psi_o^2\zeta^2\right]^{\mu/2}\left[P_\nu^\mu(\psi_o\zeta) + P_\nu^\mu(-\psi_o\zeta)\right]d\zeta \qquad \text{(A4)}$$

Now we have a special case of a hypergeometric function as[1A, 2A]

$$\left[1 - \psi_o^2\zeta^2\right]^{\frac{1}{2}\left(\frac{1}{2}-\alpha-\beta\right)}\left[P^{\frac{1}{2}-\alpha-\beta}_{\alpha-\beta-\frac{1}{2}}(\psi_o\zeta) + P^{\frac{1}{2}-\alpha-\beta}_{\alpha-\beta-\frac{1}{2}}(-\psi_o\zeta)\right]$$

$$= \frac{\pi^{1/2}2^{\frac{3}{2}-\alpha-\beta}}{\Gamma\left(\frac{1}{2}+\alpha\right)\Gamma\left(\frac{1}{2}+\beta\right)}F\left(\alpha,\ \beta;\ \frac{1}{2};\ \psi_o^2\zeta^2\right) \qquad \text{(A5)}$$

for $0 < \psi_o^2\zeta^2 < 1$. Let

$$\mu \equiv \frac{1}{2} - \alpha - \beta\ , \qquad \nu = \alpha - \beta - \frac{1}{2} \qquad \text{(A6)}$$

giving

$$\alpha = \frac{\nu - \mu + 1}{2}\ , \qquad \beta = -\frac{\nu + \mu}{2} \qquad \text{(A7)}$$

and

$$\left[1 - \psi_o^2\zeta^2\right]^{\mu/2}\left[P_\nu^\mu(\psi_o\zeta) + P_\nu^\mu(-\psi_o\zeta)\right]$$

$$= \frac{\pi^{1/2}2^{\mu+1}}{\Gamma\left(\frac{1}{2}+\beta\right)\Gamma\left(\frac{1}{2}+\alpha\right)}F\left(\beta,\ \alpha;\ \frac{1}{2};\ \psi_o^2\zeta^2\right)$$

1A. Ref. 6, eqn. 15.4.23.

2A. Ref. 9, p. 53.

$$= \frac{\pi^{1/2} 2^{\mu+1}}{\Gamma\left(\frac{1}{2} - \frac{\mu}{2} - \frac{\nu}{2}\right)\Gamma\left(1 - \frac{\mu}{2} + \frac{\nu}{2}\right)} F\left(-\frac{\mu+\nu}{2}, \frac{1-\mu+\nu}{2}; \frac{1}{2}; \psi_o^2\zeta^2\right) \qquad \text{(A8)}$$

This then gives

$$\Xi_1 = \frac{\pi^{1/2} 2^{\mu+1}}{\Gamma\left(\frac{1}{2} - \frac{\mu}{2} - \frac{\nu}{2}\right)\Gamma\left(1 - \frac{\mu}{2} + \frac{\nu}{2}\right)} \int_o^1 [1-\zeta^2]^{\lambda-1} F\left(-\frac{\mu+\nu}{2}, \frac{1-\mu+\nu}{2}; \frac{1}{2}; \psi_o^2\zeta^2\right) d\zeta \qquad \text{(A9)}$$

The hypergeometric function is given by

$$F(\alpha, \beta; \gamma; z) = F(\beta, \alpha; \gamma; z) \equiv \sum_{q=o}^{\infty} \frac{(\alpha)_q (\beta)_q}{(\gamma)_q} \frac{z^q}{q!} \qquad \text{(A10)}$$

where the Pochhammer symbol[3A] is defined by

$$(\alpha)_o \equiv 1$$

$$(\alpha)_q = \alpha(\alpha + 1)(\alpha + 2) \cdots (\alpha + q - 1) \qquad \text{(A11)}$$

and provided α is not a negative integer or zero

$$(\alpha)_q = \frac{\Gamma(\alpha + q)}{\Gamma(\alpha)} \qquad \text{(A12)}$$

Then we have the integral

$$\Xi_2 \equiv \int_o^1 [1-\zeta^2]^{\lambda-1} F\left(-\frac{\mu+\nu}{2}, \frac{1-\mu+\nu}{2}; \frac{1}{2}; \psi_o^2\zeta^2\right) d\zeta$$

$$= \sum_{q=o}^{\infty} \frac{\left(-\frac{\mu+\nu}{2}\right)_q \left(\frac{1-\mu+\nu}{2}\right)_q}{\left(\frac{1}{2}\right)_q} \frac{\psi_o^{2q}}{q!} \int_o^1 [1-\zeta^2]^{\lambda-1} \zeta^{2q} d\zeta \qquad \text{(A13)}$$

3A. Ref. 6, eqn. 6.1.22.

This leaves us with the integral (in which we let $\xi = \zeta^2$) as

$$\Xi_3 \equiv \int_o^1 [1 - \zeta^2]^{\lambda-1} \zeta^{2q} d\zeta$$

$$= \frac{1}{2}\int_o^1 [1 - \xi]^{\lambda-1} \xi^{q-\frac{1}{2}} d\xi$$

$$= \frac{1}{2} B\left(\lambda, q + \frac{1}{2}\right) = \frac{1}{2} \frac{\Gamma(\lambda)\Gamma\left(q + \frac{1}{2}\right)}{\Gamma\left(\lambda + q + \frac{1}{2}\right)} \tag{A14}$$

where B is the well known beta function and we need $Re[\lambda] > 0$.

Recombining these terms gives

$$\Xi_2 = \frac{\Gamma\left(\frac{1}{2}\right)\Gamma(\lambda)}{2\Gamma\left(\lambda + \frac{1}{2}\right)} \sum_{q=o}^{\infty} \frac{\left(-\frac{\mu+\nu}{2}\right)_q \left(\frac{1-\mu+\nu}{2}\right)_q}{\left(\lambda + \frac{1}{2}\right)_q} \frac{\psi_o^{2q}}{q!}$$

$$= \frac{\pi^{1/2}\Gamma(\lambda)}{2\Gamma\left(\lambda + \frac{1}{2}\right)} F\left(-\frac{\mu+\nu}{2}, \frac{1-\mu+\nu}{2}; \lambda + \frac{1}{2}; \psi_o^2\right) \tag{A15}$$

and then

$$\Xi_1 = \frac{\pi 2^{\mu}\Gamma(\lambda)}{\Gamma\left(\lambda + \frac{1}{2}\right)\Gamma\left(\frac{1}{2} - \frac{\mu}{2} - \frac{\nu}{2}\right)\Gamma\left(1 - \frac{\mu}{2} + \frac{\nu}{2}\right)} F\left(-\frac{\mu+\nu}{2}, \frac{1-\mu+\nu}{2}; \lambda + \frac{1}{2}; \psi_o^2\right) \tag{A16}$$

This result for Ξ_1 is very similar to a formula in a standard reference.[4A] However, in the course of our present investigations we found this formula to be in error, most likely through a misprint. This led us to do the above derivation to find the correct formula. We would like to thank Prof. Fritz Oberhettinger of Oregon State University for our discussions with him on this problem.

4A. A. Erdelyi, ed., Tables of Integral Transforms, Vol. 2, McGraw Hill, 1954, p. 318, eqn. 31.

In equations A2 and A16 let

$$\lambda \equiv \frac{1}{2}, \qquad \mu \equiv 1, \qquad \nu \equiv n \tag{A17}$$

Then we have

$$\Lambda_n = \frac{1}{\pi} \Xi_1$$

$$= \frac{2\Gamma\left(\frac{1}{2}\right)}{\Gamma\left(-\frac{n}{2}\right)\Gamma\left(\frac{n+1}{2}\right)} F\left(-\frac{n+1}{2}, \frac{n}{2}; 1; \psi_o^2\right) \tag{A18}$$

Since (n+1)/2 is a positive integer we have

$$\Gamma\left(\frac{n+1}{2}\right) = \left(\frac{n-1}{2}\right)! = \frac{(n-1)!!}{2^{\frac{n-1}{2}}} \tag{A19}$$

$$\frac{\Gamma\left(\frac{1}{2}\right)}{\Gamma\left(-\frac{n}{2}\right)} = \left(-\frac{n}{2}\right)\left(-\frac{n}{2}+1\right) \cdots \left(-\frac{1}{2}\right) = \frac{(-1)^{\frac{n+1}{2}}}{2^{\frac{n+1}{2}}} n!!$$

This gives

$$\Lambda_n = (-1)^{\frac{n+1}{2}} \frac{n!!}{(n-1)!!} F\left(-\frac{n+1}{2}, \frac{n}{2}; 1; \psi_o^2\right) \tag{A20}$$

Using equation 71 this can be written

$$\Lambda_n = P_n^1(0) F\left(-\frac{n+1}{2}, \frac{n}{2}; 1; \psi_o^2\right) \tag{A21}$$

Writing out the series we have

$$\Lambda_n = P_n^1(0) \sum_{q=0}^{\frac{n+1}{2}} \frac{\left(-\frac{n+1}{2}\right)_q \left(\frac{n}{2}\right)_q}{(q!)^2} \psi_o^{2q} \qquad \text{(A22)}$$

Note that since (n+1)/2 is a positive integer the series in equation A22 has only a finite number of terms, making Λ_n a polynomial in ψ_o.

Appendix B: Properties of Admittance Series for Large n

The most difficult parts of the sensor response functions to calculate are the internal and external admittances because of the slow convergence of the series. In this appendix we consider the behavior of these series for large n.

From equation 105 the normalized internal admittance is

$$y_{int} = \sum_{n=1}^{\infty,2} i\pi \frac{2n+1}{n(n+1)} \left[P_n^1(0)\right]^2 F\left(-\frac{n+1}{2}, \frac{n}{2}; 1; \psi_o^2\right) \frac{kaj_n(ka)}{[kaj_n(ka)]'} \tag{B1}$$

and from equation 110 the normalized external admittance is

$$y_{ext} = \sum_{n=1}^{\infty,2} (-i)\pi \frac{2n+1}{n(n+1)} \left[P_n^1(0)\right]^2 F\left(-\frac{n+1}{2}, \frac{n}{2}; 1; \psi_o^2\right) \frac{kah_n^{(2)}(ka)}{\left[kah_n^{(2)}(ka)\right]'} \tag{B2}$$

where from equation 71 we have

$$P_n^1(0) = (-1)^{\frac{n+1}{2}} \frac{n!!}{(n-1)!!} \quad \text{for n odd} \tag{B3}$$

Define the individual terms in the summation for y_{int} as y_{int_n} and in the summation for y_{ext} as y_{ext_n} so that equations B1 and B2 can be rewritten as

$$y_{int} = \sum_{n=1}^{\infty,2} y_{int_n} \tag{B4}$$

and

$$y_{ext} = \sum_{n=1}^{\infty,2} y_{ext_n} \tag{B5}$$

Define

$$n_1 \equiv n_2 - 2 > 0 \tag{B6}$$

where n_1 and n_2 are odd integers. Then write the normalized admittances as

$$y_{int} = \sum_{n=1}^{n_1,2} y_{int_n} + \Delta_{int}$$

$$y_{ext} = \sum_{n=1}^{n_1,2} y_{int_n} + \Delta_{ext} \tag{B7}$$

Then Δ_{int} and Δ_{ext} are the errors introduced by truncating the two series with last terms given by $n = n_1$. These error terms are written as

$$\Delta_{int} = \sum_{n=n_2}^{\infty,2} y_{int_n}$$

$$\Delta_{ext} = \sum_{n=n_2}^{\infty,2} y_{ext_n} \tag{B8}$$

In this appendix we consider the individual terms in the sums and the error terms for large n.

Consider the parts of the individual terms in the admittance sums. Define an integer as

$$N = \frac{n + 1}{2} \tag{B9}$$

where only odd $n > 0$ are of interest. For the hypergeometric function we have

$$F_n \equiv F\left(-\frac{n+1}{2}, \frac{n}{2}; 1; \psi_o^2\right) = F\left(-N, N - \frac{1}{2}; 1; \psi_o^2\right)$$

$$= \sum_{q=o}^{\frac{n+1}{2}} \frac{\left(-\frac{n+1}{2}\right)_q \left(\frac{n}{2}\right)_q}{(q!)^2} \psi_o^{2q}$$

$$= \sum_{q=o}^{N} \frac{(-N)\left(N - \frac{1}{2}\right)_q}{(q!)^2} \psi_o^{2q} \qquad \text{(B10)}$$

Now this particular hypergeometric function can be written as a Jacobi polynomial using[1B]

$$F(-N,\ \alpha+1+\beta+N;\ \alpha+1;\ x) = \frac{N!}{(\alpha+1)_N} P_N^{(\alpha,\beta)}(1 - 2x) \qquad \text{(B11)}$$

which gives

$$F_n = P_N^{\left(0,-\frac{3}{2}\right)}\left(1 - 2\psi_o^2\right) \qquad \text{(B12)}$$

The Jacobi polynomials can be written as[2B]

$$P_N^{(\alpha,\beta)}(x) = 2^{-N} \sum_{q=o}^{N} \binom{N+\alpha}{q} \binom{N+\beta}{N-q} (x - 1)^{N-q} (x + 1)^q \qquad \text{(B13)}$$

where binomial coefficients are given by

$$\binom{N+\alpha}{q} = \frac{\Gamma(N + \alpha + 1)}{q!\,\Gamma(N + \alpha - q + 1)} = \frac{(N + \alpha - q + 1)_q}{q!}$$

$$\binom{N+\beta}{N-q} = \frac{\Gamma(N + \beta + 1)}{(N - q)!\,\Gamma(q + \beta + 1)} = \frac{(q + \beta + 1)_{N-q}}{(N - q)!} \qquad \text{(B14)}$$

The hypergeometric function of interest can then also be written

$$F_n = 2^{-N} \sum_{q=o}^{N} \binom{N}{q} \binom{N - \frac{3}{2}}{N-q} \left(-2\psi_o^2\right)^{N-q} \left(2 - 2\psi_o^2\right)^q$$

1B. Ref. 6, eqn. 15.4.6.

2B. Ref. 9, p. 211.

$$= \sum_{q=o}^{N} (-1)^{N-q} \binom{N}{q} \binom{N - \frac{3}{2}}{N-q} \left(\psi_o^2\right)^{N-q} \left(1 - \psi_o^2\right)^q \qquad \text{(B15)}$$

Note that the Jacobi polynomial in equation B13 is a polynomial function of both α and β as well as its argument; the same is true of the hypergeometric function in equation B11. The range of α and β are often restricted to $\alpha > -1$ and $\beta > -1$ in order to make the weight functions integrable.[3B] However we are not concerned here with the orthogonality properties of the Jacobi polynomials. Since the Jacobi polynomials are polynomial functions of α and β, as is the hypergeometric function, then both series are identical for all α and β. Thus $\beta = -(3/2)$ is allowed for the series represented in equation B15.

With the hypergeometric function represented as a Jacobi polynomial we look at the asymptotic form for large N (implying large n) of the Jacobi polynomials. As $N \to \infty$ for $0 < \zeta < \pi$ we have[4B]

$$P_N^{(\alpha,\beta)}(\cos(\zeta)) = \frac{\cos\left[\left(N + \frac{1}{2}(\alpha+\beta+1)\right)\zeta - \frac{\pi}{4}(1+2\alpha)\right]}{(\pi N)^{1/2}\left[\sin\left(\frac{\zeta}{2}\right)\right]^{\alpha+\frac{1}{2}}\left[\cos\left(\frac{\zeta}{2}\right)\right]^{\beta+\frac{1}{2}}} + O\left(N^{-\frac{3}{2}}\right) \qquad \text{(B16)}$$

Set

$$\cos(\zeta) \equiv 1 - 2\psi_o^2 \qquad \text{(B17)}$$

giving

$$\sin\left(\frac{\zeta}{2}\right) = \left[\frac{1 - \cos(\zeta)}{2}\right]^{1/2} = \psi_o$$

$$\cos\left(\frac{\zeta}{2}\right) = \left[\frac{1 + \cos(\zeta)}{2}\right]^{1/2} = \left[1 - \psi_o^2\right]^{1/2} \qquad \text{(B18)}$$

3B. A. Erdelyi, ed., Higher Transcendental Functions, Vol. 2, McGraw Hill, 1953, p. 168.

4B. Ref. 9, p. 216.

Applying this to equation B12 for $0 < \psi_o < 1$ gives as $n \to \infty$

$$F_n = \frac{\left[1-\psi_o^2\right]^{1/2}}{[\pi N \psi_o]^{1/2}} \cos\left[\left(N - \frac{1}{4}\right)\arccos\left(1-2\psi_o^2\right) - \frac{\pi}{4}\right] + O\left(n^{-\frac{3}{2}}\right) \qquad \text{(B19)}$$

Thus as $n \to \infty$ the envelope of F_n falls off proportional to $n^{-(1/2)}$. Also note as $\psi_o \to 0$ we have

$$\arccos\left(1 - 2\psi_o^2\right) = 2\psi_o + O\left(\psi_o^3\right) \qquad \text{(B20)}$$

As a check F_n was calculated from equation B10 and the asymptotic form in equation B19 was observed to approach the calculated values for large n and for values of ψ_o used for the graphs.

Now turn to the Legendre function. As $\nu \to \infty$ for fixed μ and $0 < \zeta < \pi$ we have[5B]

$$P_\nu^\mu(\cos(\zeta)) = \frac{\Gamma(\nu+\mu+1)}{\Gamma\left(\nu + \frac{3}{2}\right)}\left(\frac{\pi}{2}\sin(\zeta)\right)^{-1/2}\cos\left[\left(\nu + \frac{1}{2}\right)\zeta - \frac{\pi}{4} + \frac{\mu\pi}{2}\right] + O(\nu^{-1}) \qquad \text{(B21)}$$

Thus as $n \to \infty$ and remembering that n is odd we have

$$P_n^1(0) = \frac{\Gamma(n+2)}{\Gamma\left(n + \frac{3}{2}\right)}\left(\frac{2}{\pi}\right)^{1/2}\cos\left[(n+1)\frac{\pi}{2}\right] + O(n^{-1})$$

$$= (-1)^{\frac{n+1}{2}}\left(\frac{2}{\pi}\right)^{1/2}\frac{\Gamma(n+2)}{\Gamma\left(n + \frac{3}{2}\right)} + O(n^{-1}) \qquad \text{(B22)}$$

The gamma functions have an asymptotic form known as the Stirling approximation[6B] which has as $\nu \to \infty$

5B. Ref. 6, eqn. 8.10.7.

6B. Ref. 6, eqn. 6.1.37.

$$\Gamma(\nu) = e^{-\nu}\, \nu^{\nu-\frac{1}{2}}\, (2\pi)^{1/2}[1 + O(\nu^{-1})] \tag{B23}$$

Applying this to the gamma functions in equation B22 gives as $n \to \infty$

$$\frac{\Gamma(n+2)}{\Gamma\left(n+\frac{3}{2}\right)} = \frac{e^{-n-2}(n+2)^{n+\frac{3}{2}}}{e^{-n-\frac{3}{2}}\left(n+\frac{3}{2}\right)^{n+1}}[1 + O(n^{-1})]$$

$$= e^{-\frac{1}{2}}\, e^{\left(n+\frac{3}{2}\right)\ln(n+2)}\; e^{-(n+1)\ln\left(n+\frac{3}{2}\right)}[1 + O(n^{-1})]$$

$$= \exp\left\{(n+1)\ln\left(\frac{n+2}{n+\frac{3}{2}}\right) + \frac{1}{2}\ln(n+2) - \frac{1}{2}\right\}[1 + O(n^{-1})]$$

$$= \exp\left\{(n+1)\left[\frac{1/2}{n+\frac{3}{2}} + O(n^{-2})\right] + \frac{1}{2}\ln(n+2) - \frac{1}{2}\right\}[1 + O(n^{-1})]$$

$$= \exp\left|\ln[(n+2)^{1/2}] + O(n^{-1})\right|[1 + O(n^{-1})]$$

$$= (n+2)^{1/2}\, e^{O(n^{-1})}[1 + O(n^{-1})]$$

$$= n^{1/2}[1 + O(n^{-1})] \tag{B24}$$

Thus for the Legendre function as $n \to \infty$ we have

$$P_n^1(0) = (-1)^{\frac{n+1}{2}}\left(\frac{2}{\pi}\right)^{1/2} n^{1/2}[1 + O(n^{-1})] \tag{B25}$$

$$\left[P_n^1(0)\right]^2 = \frac{2}{\pi}\, n[1 + O(n^{-1})]$$

Next are the Bessel functions. As $n \to \infty$ we have

$$\frac{kaj_n(ka)}{[kaj_n(ka)]'} = \left\{\frac{(ka)^{n+1}}{(2n+1)!!}[1 + O(n^{-1})]\right\}\left\{\frac{(n+1)(ka)^n}{(2n+1)!!}[1 + O(n^{-1})]\right\}^{-1}$$

$$= \frac{ka}{n+1}[1 + O(n^{-1})]$$

$$= \frac{ka}{n}[1 + O(n^{-1})] \qquad \text{(B26)}$$

and

$$\frac{kah_n^{(2)}(ka)}{\left[kah_n^{(2)}(ka)\right]'} = \left\{\frac{i(2n-1)!!}{(ka)^n}[1 + O(n^{-1})]\right\}\left\{(-n)\ \frac{i(2n-1)!!}{(ka)^{n+1}}[1 + O(n^{-1})]\right\}^{-1}$$

$$= -\frac{ka}{n}[1 + O(n^{-1})] \qquad \text{(B27)}$$

Now we can consider the terms in the sums for the normalized admittances. As $n \to \infty$ we have

$$y_{int_n} = i\pi\ \frac{2n+1}{n(n+1)}\ \frac{2}{\pi}\ n[1 + O(n^{-1})]\ \frac{ka}{n}\ [1 + O(n^{-1})]$$

$$\cdot \left\{\frac{\left[1-\psi_o^2\right]^{1/2}}{[\pi N\psi_o]^{1/2}} \cos\left[\left(N - \frac{1}{4}\right)\arccos\left(1-2\psi_o^2\right) - \frac{\pi}{4}\right] + O\left(n^{-\frac{3}{2}}\right)\right\}$$

$$= i\ \frac{4ka}{n}[1 + O(n^{-1})]\left[1 - \psi_o^2\right]^{1/2}\left[\frac{2}{\pi n\psi_o}\right]^{1/2}$$

$$\cdot \left\{\cos\left[\left(\frac{n}{2} + \frac{1}{4}\right)\arccos\left(1 - 2\psi_o^2\right) - \frac{\pi}{4}\right] + O(n^{-1})\right\}$$

$$= i\,\frac{4ka}{n}\left[1-\psi_o^2\right]^{1/2}\left[\frac{2}{\pi n\psi_o}\right]^{1/2}\cos\left[\left(\frac{n}{2}+\frac{1}{4}\right)\arccos\left(1-2\psi_o^2\right) - \frac{\pi}{4}\right] + O\left(n^{-\frac{5}{2}}\right) \tag{B28}$$

This last result is also the asymptotic form for y_{ext_n} for large n. Thus the individual terms in the sums fall off like $n^{-3/2}$ for large n.

Equation B8 gives the truncation error in stopping the admittance sums at $n = n_1$. Define an upper bound for these errors by

$$\Delta_1 \geq \max(|\Delta_{int}|,\ |\Delta_{ext}|) \tag{B29}$$

Using the asymptotic form developed in equation B28 we can give an approximate value for Δ_1 by setting the cosine to one and summing the magnitude of the dominant term giving

$$\Delta_1 \simeq 4ka\left[1 - \psi_o^2\right]^{1/2}\left[\frac{2}{\pi\psi_o}\right]^{1/2} \sum_{n=n_2}^{\infty,2} n^{-\frac{3}{2}} \tag{B30}$$

Replacing the sum by an integral we have

$$\Delta_1 \simeq 4ka\left[1 - \psi_o^2\right]^{1/2}\left[\frac{2}{\pi\psi_o}\right]^{1/2} \frac{1}{2}\int_{n_2}^{\infty} \nu^{-\frac{3}{2}}\, d\nu$$

$$= 4ka\left[1 - \psi_o^2\right]^{1/2}\left[\frac{2}{\pi\psi_o}\right]^{1/2} n_2^{-\frac{1}{2}}$$

$$= 4ka\left[1 - \psi_o^2\right]^{1/2}\left[\frac{2}{\pi\psi_o n_2}\right]^{1/2} \tag{B31}$$

which for small ψ_o is

$$\Delta_1 \simeq 4ka\left[\frac{2}{\pi\psi_o n_2}\right]^{1/2} \tag{B32}$$

Actually this is a rather large overestimate of the truncation error since the cosine function alternates in sign and it was replaced by one.

Appendix C: Numerical Techniques for Computer Calculations

Joe P. Martinez, Dikewood

The numerical results plotted in figures 4 and 6 through 14 were calculated using the Control Data Corporation 6600 Computer in the Air Force Weapons Laboratory at Kirtland AFB.

The calculations for the short-circuit current transfer function and the admittances included the use of the spherical Bessel functions. These functions were computed by using both forward and backward recurrence techniques. During the initial attempts at producing the Bessel functions of the first kind, the $j_n(ka)$, machine round-off error was encountered with the use of the forward recurrence relationship as well as by series representation. Backward recurrence was found to be one solution in overcoming this problem. In using this technique, where N is the largest order desired, the (N + 6)th function is set equal to zero, the (N + 5)th function is set equal to 10^{-50}, and the recurrence relationship,

$$j_{n-1}(ka) = \frac{2n + 1}{ka} j_n(ka) - j_{n+1}(ka) \tag{C1}$$

is then used to determine the functions to n = 1. A ratio of the exact value to the calculated value at n = 1 is taken and all the calculated values to n = N are multiplied by this ratio. The Bessel functions of the second kind, $y_n(ka)$, are calculated by finding the first two orders and then applying the recurrence relationship

$$y_{n+1}(ka) = \frac{2n + 1}{ka} y_n(ka) - y_{n-1}(ka) \tag{C2}$$

By comparing the values produced by these methods against tables found in handbooks, it was determined that accuracy to eight significant figures was obtained over the range of n and ka used in the computations for this note.

Legendre functions of order 1 are used in the calculations of equation 72. These were calculated by computing the functions of degree 1 and 2 and then applying the recurrence formula

$$P^1_{n+1}(x) = \left(2 + \frac{1}{n}\right) x\, P^1_n(x) - \left(1 + \frac{1}{n}\right) P^1_{n-1}(x) \tag{C3}$$

where $x = \cos(\theta_1)$. Results obtained by this method were compared with handbook tables and with calculations done by series representations and backward recurrence. These values were found to be

accurate to eight significant figures for the range of n used in the computations.

While performing the calculations for the short-circuit current transfer function (equation 72) it was determined that the series was a rapidly converging one and that it met the ratio test for convergence. This meant that an upper bound on the absolute error could be expressed as[1C]

$$\varepsilon \leq \frac{|a_{N-2}|^2}{|a_{N-2}| - |a_N|} \tag{C4}$$

where a_N is the last term included in the summation. As explained in Section IV, only the odd-numbered n are included in the summation. The relative error will then be

$$\varepsilon_r = \left|\frac{2\varepsilon}{T}\right| \leq E \tag{C5}$$

In the calculations, E was set at .001. The number of terms necessary to satisfy this criterion varied with ka, the larger values requiring more terms. Generally the error criterion was satisfied in fewer than 100 orders (50 terms).

The calculation of the y_{int} and y_{ext} sums (equations 105 and 110) were handled in a different manner than that of the T sum due to their slow convergence. The behavior of the expressions involving the spherical Bessel functions and the hypergeometric function were studied separately to determine how the numerical calculations could be made.

It was shown in appendix B that, as $n \to \infty$

$$\frac{kaj_n(ka)}{[kaj_n(ka)]'} \to \frac{ka}{n+1} \tag{C6}$$

and

$$\frac{kah_n^{(2)}(ka)}{\left[kah_n^{(2)}(ka)\right]'} \to -\frac{ka}{n} \tag{C7}$$

1C. W. Kaplan, Advanced Calculus, Addison-Wesley, 1952, pp. 328, 329.

Numerical calculations were made in order to determine at what point the asymptotic forms of these expressions could be used with minimum loss of accuracy. It was desirable to switch to the asymptotic form at some point to avoid round-off numerical errors due to the extremely small magnitude of the $j_n(ka)$ at large n. It was found that at $n \approx 10|ka| + 30$ the asymptotic forms may be used, with a relative error of .03% at ka = 1.0 introduced in the terms. Of course, as n gets larger this error will diminish with each term.

In performing the numerical calculations for the hypergeometric function of equations 105 and 110 it was found that numerical round-off error was introduced after the sum of equation 103 was carried to a large number of terms, the number depending on ψ_o. Going to double precision on the computer greatly improved the situation, as now the number of usable values was doubled. But, the round-off errors were still introduced before the y_{int} and y_{ext} sums could be completed. As was mentioned in appendix B, the asymptotic form (equation B19) approaches F_n for large n. So it was decided to switch to this form just before the numerical errors started to be significant. Table C1 is a summary of the pertinent values which occur immediately before the switch-over points.

ψ_o	$\frac{n+1}{2}$	$F\left(-\frac{n+1}{2}, \frac{n}{2}; 1; \psi_o^2\right)$	Asymptotic Formula	Absolute Difference	Relative Difference (Percent)
.001	24999	.055569	.055816	.000246	.443453
.01	3199	.093564	.093394	.000170	.182042
.1	319	.095720	.096555	.000835	.872126

Table C1. Values of the hypergeometric function one term before the switch-over point

Now that methods have been established to calculate the terms involving the Bessel functions and the hypergeometric function, the calculation of the y_{int} and y_{ext} sums may proceed. At some n_1 a switch to the asymptotic forms of equations C6 and C7 takes place, so that equation 105 becomes

$$y_{int} = i\pi\left[\sum_{n=1}^{n_1,2} \frac{2n+1}{n(n+1)}\left[\frac{n!!}{(n-1)!!}\right]^2 F\left(-\frac{n+1}{2}, \frac{n}{2}; 1; \psi_o^2\right)\frac{kaj_n(ka)}{[kaj_n(ka)]'}\right.$$

$$\left. + ka\sum_{n=n_1+2}^{\infty,2} \frac{2n+1}{n}\left[\frac{n!!}{(n+1)!!}\right]^2 F\left(-\frac{n+1}{2}, \frac{n}{2}; 1; \psi_o^2\right)\right] \qquad \text{(C8)}$$

Similarly, equation 110 becomes

$$y_{ext} = i\pi\left[-\sum_{n=1}^{n_1,2}\frac{2n+1}{n(n+1)}\left[\frac{n!!}{(n-1)!!}\right]^2 F\left(-\frac{n+1}{2},\ \frac{n}{2};\ 1;\ \psi_o^2\right)\frac{kah_n^{(2)}(ka)}{\left[kah_n^{(2)}(ka)\right]'}\right.$$

$$\left. + ka\sum_{n=n_1+2}^{\infty,2}\frac{2n+1}{n+1}\left[\frac{(n-2)!!}{(n-1)!!}\right]^2 F\left(-\frac{n+1}{2},\ \frac{n}{2};\ 1;\ \psi_o^2\right)\right] \qquad (C9)$$

Since the switch-over occurs when $n \geq 10|ka| + 30$, and the largest value of ka used in these calculations was 10.0, all changeovers to the asymptotic forms will take place by $n > 131$. It was found to be convenient to calculate the sums, with $i\pi ka$ factored out, from n = 201 to ∞ (n odd) first, and then include these values in the calculations later. Since ka can be factored out from the last part of the summation, these values may be used with any ka. The next problem was that of determining how far n should be carried. This was done numerically by running the sums out progressively further to larger n and noting the relative change. The sums for all ψ_o were carried to n = 100001 and it was noted that they were still changing about 1 part in 1000, or .1%. It was further noted that there were peaks and minimums occurring as the sum progressed, forming a diminishing envelope converging at some number. The last few maxima and minima were then taken and the value to which they were converging was extrapolated to 5 significant digits. Table C2 gives these values. The relative error in the sum is then in the order of .05%. This error is, of course, multiplied by πka when the sums are used in the admittance calculations.

ψ_o	$(i\pi ka)^{-1}\sum_{n=201}^{\infty,2} y_{int_n}$	$(i\pi ka)^{-1}\sum_{n=201}^{\infty,2} y_{ext_n}$
.001	1.0987×10^{0}	1.1013×10^{0}
.01	-8.6355×10^{-2}	-8.6605×10^{-2}
.1	-2.0147×10^{-3}	-2.0234×10^{-3}

Table C2. Values to which admittance sums converge from n = 201, with $i\pi ka$ factored out

Most of the other numerical calculations performed for the graphs in this note are straight forward and no explanation is required.